Geochemistry, Geophysics, Geosystems

RESEARCH ARTICLE
10.1029/2020GC009481

Organic Biogeochemistry in West Mata, NE Lau Hydrothermal Vent Fields

H.-T. Lin[1,2], D. A. Butterfield[3], E. T. Baker[4,5], J. A. Resing[3], J. A. Huber[6,7], and J. P. Cowen[2,†]

[1]Institute of Oceanography, National Taiwan University, Taipei City, Taiwan, [2]Department of Oceanography, School of Ocean and Earth Science and Technology, University of Hawaii, Honolulu, HI, USA, [3]Joint Institute for the Study of the Atmosphere and Ocean, NOAA-Pacific Marine Environmental Laboratory and the University of Washington, Seattle, WA, USA, [4]Pacific Marine Environmental Laboratory, NOAA, Seattle, WA, USA, [5]Now at Joint Institute for the Study of the Atmosphere and Ocean, NOAA-Pacific Marine Environmental Laboratory and the University of Washington, Seattle, WA, USA, [6]Woods Hole Oceanographic Institution, Woods Hole, MA, USA, [7]Josephine Bay Paul Center, Marine Biological Laboratory, Woods Hole, MA, USA

†Deceased.

Key Points:

- Unique stable carbon isotope of suspended particulate organic carbon is indicative of unique carbon fixation pathway by vent biomes
- We estimated first dissolved organic nitrogen for hydrothermal vent fluids and observed enhanced nitrogen fixation and/or denitrification
- Total dark organic carbon production within the plume matches thermodynamic prediction based on available, reducing chemical substances

Supporting Information:

Supporting Information may be found in the online version of this article.

Correspondence to:

H.-T. Lin,
tinalinht@ntu.edu.tw

Citation:

Lin, H.-T., Butterfield, D. A., Baker, E. T., Resing, J. A., Huber, J. A., & Cowen, J. P. (2021). Organic biogeochemistry in West Mata, NE Lau hydrothermal vent fields. *Geochemistry, Geophysics, Geosystems*, *22*, e2020GC009481. https://doi.org/10.1029/2020GC009481

Received 15 OCT 2020
Accepted 7 FEB 2021

Abstract The impact of submarine hydrothermal systems on organic carbon in the ocean—one of the largest fixed carbon reservoirs on Earth—could be profound. Yet, different vent sites show diverse fluid chemical compositions and the subsequent biological responses. Observations from various vent sites are to evaluate hydrothermal systems' impact on the ocean carbon cycle. A response cruise in May 2009 to an on-going submarine eruption at West Mata Volcano, northeast Lau Basin, provided an opportunity to quantify the organic matter production in a back-arc spreading hydrothermal system. Hydrothermal vent fluids contained elevated dissolved organic carbon, particulate organic carbon (POC), and particulate nitrogen (PN) relative to background seawater. The δ^{13}C-POC values for suspended particles in the diffuse vent fluids (−15.5‰ and −12.3‰) are distinct from those in background seawater (−23 ± 1‰), indicative of unique carbon synthesis pathways of the vent microbes from the seawater counterparts. The first dissolved organic nitrogen concentrations reported for diffuse vents were similar to or higher than those for background seawater. Enhanced nitrogen fixation and denitrification removed 37%–89% of the total dissolved nitrogen in the recharging background seawater in the hydrothermal vent flow paths. The hydrothermal plume samples were enriched in POC and PN, indicating enhanced biological production. The total "dark" organic carbon production within the plume matches the thermodynamic prediction based on available reducing chemical substances supplied to the plume. This research combines the measured organic carbon contents with thermodynamic modeled results and demonstrates the importance of hydrothermal activities on the water column carbon production in the deep ocean.

Plain Language Summary External energies fuel the production of organic carbon and nitrogen by living organisms. Exploring the organic compounds' concentrations and characteristics help reveal the energy flow and biogeochemical processes. Here, we investigate the marine organic matter in the submarine hot springs (hydrothermal fluids) generated by deep seawater interacting with uplifting magma caused by spreading seafloor. We surveyed the organic carbon and nitrogen contents with samples collected during a cruise in May 2009, in response to an on-going submarine eruption at West Mata Volcano, northeast Lau Basin. The submarine hot spring water, relative to background seawater, had elevated organic carbon and nitrogen with unique characters. The amount of elevated organic carbon meets our calculated values based on the energy that the hot spring brings to marine life. We conclude that the underwater hot springs fuel "dark" organic carbon production via unique carbon fixation pathways in the deep ocean.

1. Introduction

The dynamics and characteristics of organic carbon in the deep ocean potentially have profound impacts on the biological activities and the global carbon cycle (Hansell et al., 2009; Jiao et al., 2010). Marine dissolved and particulate organic carbon (DOC and POC), though operationally defined size-fractions of organic matter, play essential but distinct roles (e.g., Carlson & Hansell, 2015; Druffel et al., 1992; Griffith et al., 2012; Seymour et al., 2017). POC, composed of planktons and detritus, acts as products of biological

activities (Cauwet et al., 1997; Seymour et al., 2017), whereas the DOC, produced by excretes from organisms, lysis, POC solubility, and grazing activities, act as fuels for heterotrophic bacterial activities (e.g., Azam et al., 1983; Carlson, 2002; Ducklow & Carlson, 1992; Williams, 1970). Net productions of DOC and POC often result from temporal and spatial decoupling of its in situ biological production and consumption (Carlson, 2002; Hansell & Carlson, 2001; Honjo et al., 2008). Elevated concentrations of DOC and POC occur in areas of, or at the time of, vigorous biological activities (e.g., Carlson et al., 2000; Engel et al., 2012; Hansell & Carlson, 2001; Smith et al., 1992; Tanoue & Handa, 1979). Low DOC and low POC, such as those observed in the deep ocean, results from significantly reduced biological production in the dark ocean, accompanied by abiotic and biotic removal of DOC during thermohaline circulation (Arıstegui et al., 2002; Druffel et al., 1992).

In the deep ocean, submarine hydrothermal activities also fuel biotic and abiotic organic carbon production, evidenced by elevated DOC in hydrothermal vent systems. Lang et al. (2006) reported the first systematic survey of hydrothermal vent fluid DOC. The diffuse vents off the sedimented Endeavor and the unsedimented Axial Volcano vent fields contained DOC with concentrations of 42–69 μM and 34–71 μM, respectively (Lang et al., 2006). As a comparison, the non-vent influenced background seawater had DOC of 36 μM (Lang et al., 2006). Recently, Hawkes et al. (2015) observed significantly elevated DOC concentration up to 607 μM for a diffuse vent in the unsedimented basalt-hosted Axial Volcano with relatively low hydrogen concentration (<1 mM). They also reported DOC as high as 750 μM for a sedimented Gabbro/Peridotite-hosted focused vent (Chimlet 2) in Von Damm, Caribbean, where the hydrogen concentration was high (>10 mM). These high DOC concentrations have passed the quality check by Hawkes et al. (2015), who attributed the variable vent fluid DOC caused by the natural dynamics or random contamination from sediments, macro-, micro-fauna, or ROV operations.

Elevated suspended organic particles in hydrothermal vents and plumes also indicate production in hydrothermal systems. Comita et al. (1984) first reported that the POC and particulate nitrogen (PN) in the vent fluids and the non-vent water varied by a factor of 2–5, the higher values being in the vent fluids of the East Pacific Rise 21°N vent field. Maruyama et al. (1993) reported 5.8 to 9.2 μmol-C/L of suspended organic particles in the black smoking vent fluids off Izena, Okinawa Trough. Bennett, Statham, et al. (2011) observed increased POC concentrations (0.87–3.81 μmol/L) in the near-field diffuse vents from East Pacific Rise 9°50′N.

Nevertheless, some hydrothermal systems do not favor organic matter production. The heats, the porous rocks, and the heterotrophic organisms residing in the subsurface may indeed remove deep-ocean dissolved organic matter (DOM) effectively (Hawkes et al., 2015; Lang et al., 2006; Lin et al., 2012; Walter et al., 2018). Sediment-buried ridge flank oceanic crustal fluids contained significantly depleted DOC on the Juan de Fuca (~12 μM) and the North Pond (18–33 μM) relative to recharging background seawater (Lang et al., 2006; Lin et al., 2012, 2019; McCarthy et al., 2010; Walter et al., 2018). High-temperature focused vent fluids from mid-ocean ridges at Mean Endeavor Field, Axial Volcano, East Pacific Rise 9°50′N (Bio 9) contained 14–17 μM of DOC (Lang et al., 2006; Longnecker et al., 2018). The fractions of solid-phase extractable DOC in hydrothermal solutions during laboratory heating experiments were much less than those in deep ocean samples (Hawkes et al., 2015). These observations reinforced the importance of possible thermal alteration and removal of DOM in some hydrothermal systems.

Qualitatively, extensive seafloor and subseafloor biological and abiotic processes in hydrothermal regions should alter the composition of the organic matter. The hydrothermal ecosystem may generate organic carbon with unique stable carbon isotope compositions. Lin et al. (2019) and Walter et al. (2018) used large volume samples (1–60 L) from the warm (65°C) and cold (10°–25°C) ridge flanks, respectively, to investigate the DOC carbon isotope biogeochemistry. Lin et al. (2019) reported elevated aromatic compounds in the warm basaltic ridge flank fluids, which is likely resulted from thermal condensation reactions (Lin et al., 2019). However, organic matter characterization research often requires a large sample size (Repeta, 2015) and is thus challenging for hydrothermal studies.

Nevertheless, the organic carbon to nitrogen ratios (C/N ratios) and the stable carbon isotopic compositions ($\delta^{13}C$) with small samples (few liters) provide insights into the quality of the organic matter. Comita et al. (1984) concluded that the suspended particulate organic matter (POM) in the vent fluids with low

C/N (hereafter $C/N_{\text{-POM}}$) of 12–18 was distinct from the high $C/N_{\text{-POM}}$ (~24) for the presumably resistant and remineralized POM in non-vent water. The low C/N in vents may reflect the accumulation of fresh biomass, such as marine planktons, on average, having a C/N ratio of ~6 (Redfield, 1934, 1958). Low C/N ratios (4.1 ± 0.6) of the quantifiable suspended particles in the subseafloor ridge-flank-fluid samples (Lin et al., 2019) suggest bacterial biomass as the dominant source of POC (Fukuda et al., 1998). The carbon isotopic compositions of POC also reflect the potential carbon source and carbon assimilation pathways (e.g., Hayes, 2001; Hofmann et al., 2000; Popp et al., 1998; Preuss et al., 1989; Sirevåg et al., 1977). Autotrophs preferentially incorporate ^{12}C-depleted inorganic carbon into their biomass, leading to a low δ^{13}C-POC value in the biomass than the δ^{13}C of inorganic carbon (House et al., 2003). Microbial metabolism using isotopically light methane (Lin et al., 2014) also results in depleted δ^{13}C-POC value (−34 ± 0.1‰) in a ridge flank hydrothermal system (Lin et al., 2019).

The amounts of dissolved organic nitrogen (DON), nitrogen-containing DOC, though rarely reported, also characterize the dissolved organic matter in an aquatic environment. For example, surface seawater has elevated DON (5.1 ± 1.7 μM) than the deep sea (2–5 μM; with an average of 3.2 ± 2.2 μM, Sipler & Bronk, 2015). In productive coastal regions, the DON can be as high as 16 μM (Bronk et al., 2014; Sipler & Bronk, 2015). The C/N of DOM (hereafter, $C/N_{\text{-DOM}}$) also provide qualitative information. For instance, DOM enriched in aromatic over aliphatic compounds would have higher $C/N_{\text{-DOM}}$ (Sipler & Bronk, 2015). DOM containing elevated humic or fulvic acids would also be high in $C/N_{\text{-DOM}}$ (Bronk et al., 2007; See & Bronk, 2005). However, DON measurements are not yet available for hydrothermal fluids, likely due to methodological constraints. Some hydrothermal vent fluids, such as the ridge flank basaltic fluids from the eastern Juan de Fuca, contained ammonium as high as 100 μM (Lin et al., 2012). The DON concentrations, typically obtained by subtracting inorganic nitrogen from the total dissolved nitrogen (TDN), is as large as the analytical uncertainty.

This study overcame the sampling and analytical challenges and presented the first hydrothermal vent fluid DON measurements. We report and discuss the DOC, POC, δ^{13}C-POC, PN for diffuse vent fluids in a vent field where there was an on-going seafloor eruption. We elucidate the biogeochemical processes leading to our observation. Lastly, we investigate the amount of potential organic carbon production in the plume from the energy available by thermodynamic modeling.

2. Geological Settings and Methods

2.1. Lau Basin

The Lau Basin is a triangular-shaped active back-arc basin associated with the Tonga-Kermadec subduction zone along the western Pacific margin (Figure 1a). There are multiple rifting and spreading centers in the Lau Back-arc Basin (Hawkins, 1995; Taylor et al., 1996); the most northeastern of them is the Northeast Lau Spreading Center (NELSC). NELSC's maximum full spreading rate is estimated to be about 94 mm/year based on the value obtained from a three-plate kinematic model for Lau Basin opening (German et al., 2006; Zellmer & Taylor, 2001). Between the NELSC and the frontal magmatic arc of the Tonga-Kermadec subduction zone lie several submarine volcanoes, including the West Mata volcano (Baker et al., 2011; Embley et al., 2014). Slab subduction induced eruptions from an active proto-arc volcano (Resing et al., 2011). This entire area is hydrothermally very active (Baker et al., 2011; German et al., 2006; Resing et al., 2011). National Oceanic and Atmospheric Administration Pacific Marine Environmental Laboratory (NOAA-PMEL) detected active eruption events on both the NELSC and at West Mata in November 2008 (Baker et al., 2011; Baumberger et al., 2014; Clague et al., 2011; Embley et al., 2014; Resing et al., 2011; Rubin et al., 2012).

2.2. Response Cruise and Sampling Sites

In response to the two eruptions discovered in November 2008 (Baker et al., 2011; Clague et al., 2011; Resing et al., 2011; Rubin et al., 2012), we staged a research cruise to Northeast Lau over May 5–13, 2009 on the research vessel Thomas Thompson (Resing et al., 2011). We conducted seven dives with the remotely operated vehicle (ROV) JASON II (operated by Woods Hole Oceanographic Institution). Five dives were at the West Mata area, and two dives at the NELSC (Figure 1a). We observed active eruptions at West Mata during each dive and identified three eruption sites—Hades, Akel's Afi, and Prometheus (Resing et al., 2011). Near the

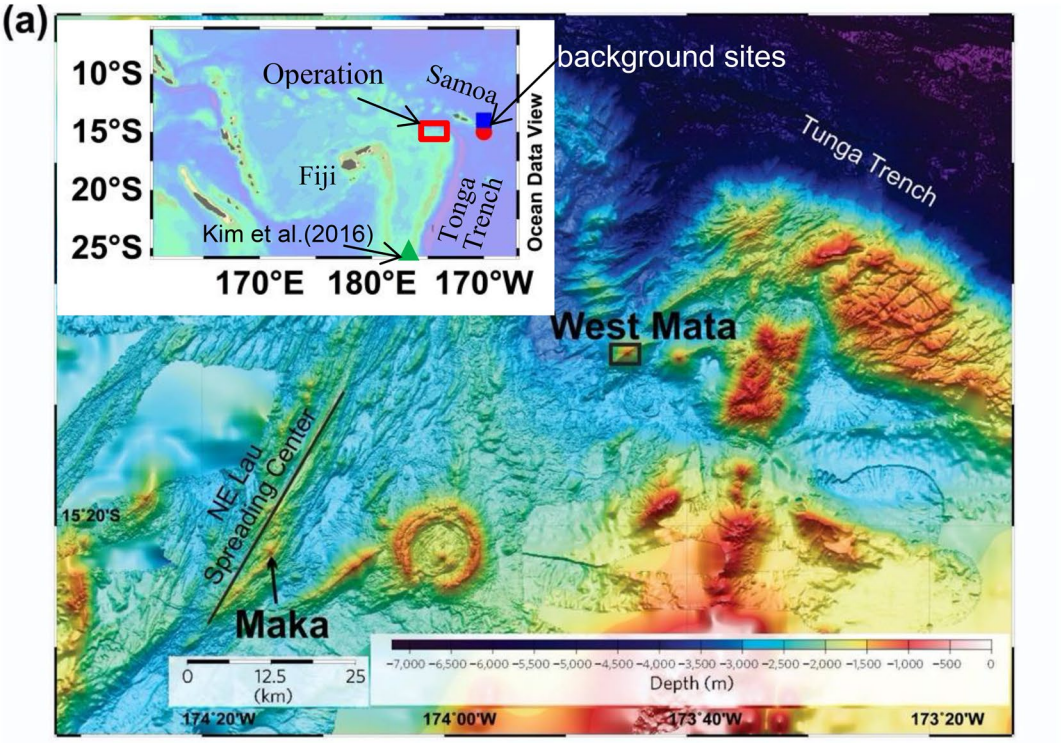
(a)
10°S
15°S
20°S
25°S
170°E 180°E 170°W
Operation
Samoa
Fiji
Tonga Trench
Kim et al.(2016)
Ocean Data View
background sites
Tunga Trench
West Mata
NE Lau Spreading Center
Maka
15°20'S
0 12.5 25 (km)
−7,000 −6,500 −6,000 −5,500 −5,000 −4,500 −4,000 −3,500 −3,000 −2,500 −2,000 −1,500 −1,000 −500 0
Depth (m)
174°20'W
174°00'W
173°40'W
173°20'W

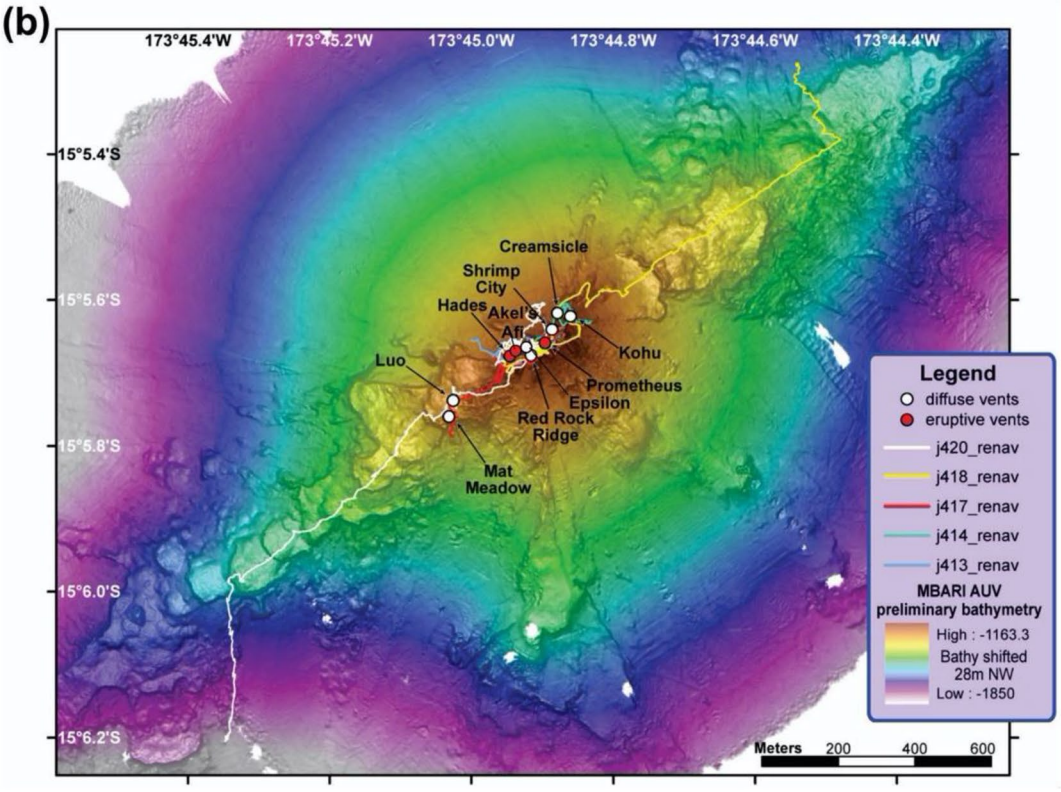
(b)
173°45.4'W
173°45.2'W
173°45.0'W
173°44.8'W
173°44.6'W
173°44.4'W
15°5.4'S
15°5.6'S
15°5.8'S
15°6.0'S
15°6.2'S
Creamsicle
Shrimp City
Hades
Akel's Afi
Kohu
Luo
Prometheus
Epsilon
Red Rock Ridge
Mat Meadow
Legend
diffuse vents
eruptive vents
j420_renav
j418_renav
j417_renav
j414_renav
j413_renav
MBARI AUV preliminary bathymetry
High : -1163.3
Bathy shifted 28m NW
Low : -1850
Meters 200 400 600

Table 1
Sampling Sites

Sampling site	JASON dive#	CTD cast #	Latitude (°S)	Longitude (°W)	Sampling depth (m)
Submergence vehicle operation					
W. Mata diffuse vents					
Creamsicle	J418	–	15.093645	173.747971	1,206
Red Rock	J413	–	15.094602	173.748589	1,183
Kohu	J414	–	15.093718	173.747666	1,188
Shrimp City	J414	–	15.094023	173.748098	1,187
Luo	J417	–	15.095635	173.750425	1,277
Epsilon	J417	–	15.094530	173.748575	1,179
W. Mata Eruptive sites					
Akel's Afi	J418	–	15.094446	173.749047	1,215
Hades	J413	–	15.094707	173.749115	1,206
CTD operation					
Vertical cast					
Above W. Mata	–	V09C01	15.094278	173.748523	949––1,148
Above Maka	–	V09C02	15.423150	174.284933	1,195––1,556
Tow-yo					
NE Lau Spreading Center	–	T09C01	15.381515	174.242577	996
NE Lau Spreading Center	–	T09C01	15.390883	174.251013	1598

eruption sites, we discovered several low-temperature diffuse vents—Creamsicle, Red Rock Ridge, Kohu, Shrimp City, Luo, and Epsilon (Table 1 and Figures 1 and 2). In contrast, we found no eruptive activity along with the NELSC (Figure 1).

We conducted several CTD-rosette operations from the research vessel, including two vertical casts (V09C01 and V09C02, Table 1) over the West Mata eruptive site and the NELSC, respectively. We made two horizontal tows during which the CTD was continuously lowered and raised in a saw-toothed pattern (i.e., tow-yos; Baker & Massoth, 1987) as water samples were collected. Sensors on the CTD rosette recorded conductivity, temperature, pressure, oxygen, optical backscatter, fluorescence, altimetry, and oxidation-reduction potential (ORP). Anomalies in ORP indicate the presence of reduced chemical species such as H_2S and Fe^{2+}.

2.3. Sampling and Analytical Methods

Plume and background seawater samples were collected with Niskin bottles during CTD-rosette vertical and tow-yo casts following the guide to ocean carbon research (Dickson et al., 2007). There is not yet a consensus protocol to collect hydrothermal fluid samples for organic carbon research. Hydrothermal fluids are usually directly collected into a bag, polyvinyl chloride (PVC), or titanium sampler (Bennett, Hansman, et al., 2011; Bennett, Statham, et al., 2011; Hawkes et al., 2015; Lang et al., 2006, 2010; Lin et al., 2012, 2019). There was no opportunity to rinse the sample storage devices during seafloor operation. Previous research pointed out that hydrothermal samples are prone to receive random DOC contamination (Hawkes et al., 2015). Thus, contamination controls on the sampling systems are crucial to using the samples for DOC research.

Figure 1. Map of the study site. (a) Regional map of NE Lau basin. The insert shows the location of the NE Lau basin relative to Fiji, Samoa, and Tonga Trench (Ocean Data View; Schlitzer et al., 2018). The red box indicates the operation area for this study and is enlarged in Figure 1a. The red circle and blue square indicate the locations of two background water column casts (15°S, 170°W; 14°S, 170°W; transect P15S of WOCE/CLIVAR http://yyy.rsmas.miami.edu/groups/biogeochem/Data.html), used for comparison to data obtained by this study. The green triangle denotes the sites for the sinking particle research by Kim et al. (2016). A black box denoted the area of West Mata enlarged in Figure 1b. (b) Detailed bathymetric map of W. Mata. Map credit: Susan Merle OSU CIMRS/NOAA EOI.

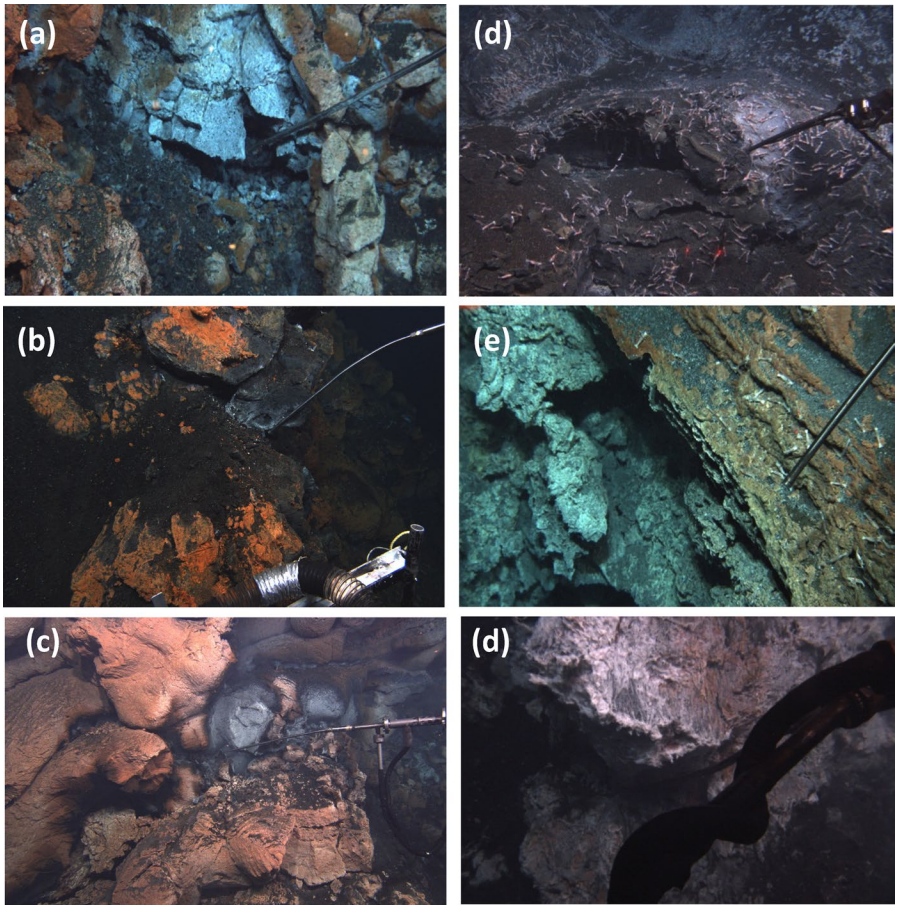

Figure 2. Sampling photos: Diffuse vents (a) Creamsicle, (b) Red Rock, (c) Kohu, (d) Shrimp City, (e) Luo, and (f) Epsilon.

For this study, hydrothermal vent fluid samples were collected via ROV JASON II using the PMEL Hydrothermal Fluid and Particulate Sampler (HFPS; Butterfield et al., 2004; Huber et al., 2006) into 800 mL Tedlar bags. The HFPS lids for the bags were cleaned and sterilized with ethanol, rinsed vigorously with deionized water, and finally rinsed with 0.2 μm filtered seawater. The DOC blank for an HFPS bag was ~1 μM, obtained by measuring the deionized water sat in the Tedlar bag for several hours. The TDN blank value for the bag was <0.5 μM. The DOC blank of the HFPS bag increased to 5.2 μM in extremely acidic conditions (0.24N HCl, pH < 1) for a prolonged period while the TDN remained undetected (<0.5 μM).

All fluid samples for DOC, TDN, and nutrient analyses were filtered shipboard through GF/F filters (25 mm; precombusted at 550°C for 5 h) in acid-cleaned Whatman® polypropylene 25 mm filter holders (Whatman International Ltd, UK). Before use, we passed at least 50 mL of deionized water through each filter to lower a DOC blank to below the detection limit (1 μM) based on our laboratory test results. The filtered samples were stored in acid-washed high-density polyethylene Nalgene bottles and kept frozen until thawed for analysis (Tupas et al., 1994).

Particulates were collected by pumping 2–5 L of hydrothermal vent fluids through combusted GF/F filters using the HFPS in situ. About 10 L of seawater collected with CTD-rosette Niskin bottles were filtered on board ship through combusted GF/F filters. Individual filters were wrapped in combusted foils and stored frozen until thawed for analysis.

DOC and TDN concentrations were measured by high-temperature (720°C) combustion using a Shimadzu TOC-V_{CSH} analyzer. Samples were acidified to pH < 2 within the autosampler syringe by adding 45 μL of 2N HCl to 3 mL samples. No acid contamination was observed throughout the analysis. The acidified

samples were purged with purified air (Shimadzu compressed air and carrier gas purification kit) to remove inorganic carbon. Five to six replicate analyses were performed using an injected sample volume of 150 μL. DOC and TDN concentrations were calibrated with gravimetrically prepared potassium hydrogen phthalate (KHP) and sodium nitrate standards. The reproducibility between replicate injections was <2 μM, that is, <5% at 40 μM. Two consensus reference materials (CRM, from University of Miami, Dickson et al., 2007), Florida Strait 700 m-deep seawater (DSW) and low carbon water (LCW), were used extensively before, between, and after sample analysis. At least one CRM was measured every five samples. The measured concentration of CRM-DSW was 42 ± 0.2 μM ($n = 23$), consistent with the certified range of DOC concentration (41–43 μM). The average measured CRM-LCW value was 1.3 ± 0.4 μM ($n = 7$), which also fell within the certified range of 1–2 μM. The detection limit was about 1 μM. TDN was measured with a chemiluminescence detector in-line with the described Shimadzu TOC-V_{CSH} analyzer (Sharp et al., 2002). Measured CRM-DSW was 33 ± 0.1 μM ($n = 23$), the same as the certified value of 33 μM. The analytical precision was 0.1 μM, and the detection limit was about 0.5 μM.

Nitrate-plus-nitrite (N + N) analysis was carried out with a custom-build colorimetric flow injection analyzer (Grasshoff et al., 1999). Sample nitrate was first reduced to nitrite with a Cu-Cd column and then analyzed as nitrite. The Cu-Cd column's reduction efficiency, the absorbance ratio of nitrate and nitrite standard at an equal concentration (e.g., 5 or 20 μM; gravimetrically prepared), was maintained at 100 ± 1%. We regenerated the Cu-Cd column with ammonium chloride between each sample to minimize possible interferences by the reducing compounds in the hydrothermal fluids. The detection limit for N + N analysis was 0.1 μM, and analytical precision was <0.05 μM. Ammonium concentrations were measured at the University of Hawaii with a flow injection-fluorometric method (Jones, 1991) and calibrated against gravimetrically prepared ammonium chloride (NH_4Cl) standards. The detection limit was 0.1 μM at the setting for measuring low concentrations of ammonium in the vent fluids. The analytical uncertainty was 0.03 μM.

Silicate was measured by colorimetry (Grasshoff et al., 1999). Samples were first diluted 100 times, reacted with acidic molybdenum, and reduced with ascorbic acid. The analytical uncertainty for the diluted samples was about 0.1 μM. Total dissolved iron (1-sigma precision 4%) in vent fluids was measured by atomic absorption at PMEL/Seattle on samples preserved shipboard with ultra-pure HCl (TraceMetal Grade). The total iron of acidified plume samples was measured by a Ferrozine colorimetry method (Gibbs, 1976; Stookey, 1970). The ferrozine method had an analytical uncertainty of 0.03 μM and a detection limit of 0.1 μM. The pH was measured shipboard at laboratory temperature in a closed vessel using a glass pH electrode (Ross Sure-Flow) calibrated with NBS-certified buffers (Fisher Scientific). The precision of the measurement is 0.02 pH units.

The POC and PN and isotopic compositions of acidified (with 1 N HCl) GF/F samples were measured with a CN elemental analyzer (Costech, ECS 4010) connected in-line with an isotope ratio mass spectrometer (IRMS; Thermo Finnigan Delta XP) interfaced with a ConFloIV, at the University of Hawaii. Isotope values are reported in conventional δ notation relative to the international standards atmospheric N_2 and V-PDB, for N and C, respectively. The detection limit for carbon and nitrogen content is 10 μg-C and 0.3 μg-N, respectively. The limit for reliable carbon and nitrogen isotopic determination is 10 μg-C and 10 μg-N, respectively. Glycine was used as the reference material for both the quantification of C and N and the isotopic correction. A homogenized tuna white muscle tissue reference was also analyzed at least triplicate as an external standard to verify instrument accuracy and precision. Our in-house reference materials were extensively characterized with certified reference materials, including NBS 18, NBS 19, NIST 1547, NIST 3, USGS 32, USGS 34, and USGS 35.

2.4. Chemoautotrophic Production Energetics

The oxidation reactions of reduced species, using Fe^{2+} as an example, can be expressed as:

$$Fe^{2+} + 1/4O_{2(aq)} + 2.5H_2O = Fe(OH)_{3(s)} + 2H^+ \quad (1)$$

The amount of energy released or required for the oxidation reactions is expressed as Gibbs free energy of reaction (ΔG_r) and is calculated as:

$$\Delta G_r = \Delta G_r^\circ + RT\ln Q \quad (2)$$

where ΔG_r° is the standard state Gibbs energy of reaction at the temperature and pressure of interest, R is the gas constant, and T is the temperature in Kelvin. Q is the reaction quotient and can be calculated as:

$$Q = \Pi\left(a_i^{v_{i,r}}\right) \quad (3)$$

where a_i denotes the activity of chemical species i, and $v_{i,r}$ is its stoichiometric coefficient in reaction r, which is negative for reactants and positive for products.

ΔG_r^0 is derived from the respective equilibrium constant (K) near in situ pressure (120 bar). The equilibrium constants at 4°C were computed using the revised H.K.F. equations of state (Helgeson et al., 1981; Shock et al., 1992; Tanger & Helgeson, 1988), the SUPCRT 92 software package (Johnson et al., 1992):

$$\Delta G_r^0 = -2.3RT\log \mathrm{K} \quad (4)$$

The Q values were calculated based on the maximum values reported for the 2008 plume (Resing et al., 2011) or the values derived from the electronic atlas of WOCE hydrographic and tracer data (Schlitzer, 2000). The activity coefficients of neutral species such as dissolved oxygen and hydrogen were assumed to be unity (McDermott et al., 2015).

3. Results

Directly measured values are reported due to the difficulty in obtaining a suitable factor for seawater entrainment correction (details in Section 4.1).

3.1. DOC, TDN, NO_3^-, NH_4^+, DON, and POC in Vent Fluid Samples

The DOC concentrations (39–521 μM) in the diffuse vent fluids from West Mata vary from close to bottom seawater values (~39 μM) at Creamsicle and Red Rock to greatly elevated values at Luo and Epsilon (Table 2). The agreement of the replicate bag samples at Creamsicle (Table 2) documents the consistency of our sampling and analytical procedures.

The elevated DOC of vent fluids from Luo at NE Lau was within the range of porewater extracted from microbial mats recovered from the Loihi vent field (68–179 μM, Bennett, Hansman, et al., 2011). The diffuse vents contained TDN concentrations of 4.3–24.5 μM, much lower than bottom seawater (39 μM). The vent fluids had NO_3^- between 1.8 and 21 μM, but background seawater had NO_3^- up to 37 μM. The vent fluids had 0.3–3.4 μM NH_4^+ whereas seawater NH_4^+ was undetectable (Table 2). The calculated DON was between 1.6 and 3.4 μM with cumulative errors of between 0.1 and 0.5 μM. The POC and PN concentrations in Red Rock and Luo diffuse vent fluid samples are an order of magnitude higher than that for background seawater (Table 3). The $\delta^{13}C$ values for the POC from Red Rock and Luo vents are −15.5‰ and −12.3‰, respectively, which is significantly enriched in ^{13}C relative to the POC in nearby background seawater (−23 ± 1‰) (Table 3).

3.2. DOC, TDN, POC, and PN in Hydrothermal Plume Samples

We identified a pronounced particle-rich layer ~80–100 m above the West Mata eruption sites as a neutrally buoyant hydrothermal plume, accompanied by anomalously high turbidity and low ORP (Table 4; Figure 3). The DOC concentrations in the neutrally buoyant plume samples above West Mata (45 ± 1 μM) are significantly higher than those of background seawater (39 ± 1 μM). TDN concentrations in plume samples above both West Mata are uniformly 39 ± 1 μM, not significantly different from those in background seawater. POC and PN concentrations, 0.45 ± 0.12 μmol-C/L and 0.043 ± 0.08 μmol-N/L (n = 4), respectively, in West Mata plume samples are higher than those in background seawater samples (0.18 ± 0.06 μmol-C/L and 0.022 ± 0.09 μmol-N/L; Table 4; Figure 4).

Table 2
Diffusive Vent Fluid and Background Seawater Biogeochemical Compositions: Maximum Temperature During Sampling (T_{max}), Equilibrated pH at 25°C, Concentrations of Magnesium (Mg), Dissolved Organic Carbon (DOC), Total Dissolved Nitrogen (TDN), Ammonium (NH_4^+), Nitrite (NO_2^-), Nitrate (NO_3^-), Calculated Dissolved Organic Nitrogen (DON = TDN−NH_4^+−NO_2^-−NO_3^-), silicate (Si), Total Dissolved Iron (TdFe), and Phosphate (PO_4^{3-})

Vent type & name	Sampler type	Tmax (°C)	pH	Mg (mM)	DOC (μM)	TDN (μM)	NH_4^+ (μM)	NO_2^- (μM)	NO_3^- (μM)	Cal. DON (μM)	C/N$_{DOM}$	DON: TDN	Si (μM)	TdFe (μM)	PO_4^{3-} (μM)
Diffusive vent															
Creamsicle	HFPS-Bag	29.3	3.0	58	39 ± 2	4.3 ± 0.1	0.3	<0.05	1.8	2.1	18	50%	2986	812	6.3
Creamsicle	HFPS-Bag	29.3	2.9	58	41 ± 5	5.8 ± 0.4	0.3	<0.05	-	-	-	-	3,104	840	5.6
Red Rock	HFPS-Bag	13.8	3.2	57	43 ± 1	24.5 ± 0.5	0.4	<0.05	21	3.0	14	12%	1,173	854	6.2
Kohu	HFPS-Bag	30.8	3.0	58	86 ± 3	13.9 ± 0.3	0.5	<0.05	10	3.4	25	25%	3,319	962	6.8
Shrimp City	HFPS-Bag	14.8	5.8	57	84 ± 2	10.8 ± 0.4	0.8	<0.05	8	2.1	40	19%	1,084	21	6.1
Luo	HFPS-Bag	22.4	5.3	55	126 ± 7	12.7 ± 0.3	3.4	<0.05	6	3.3	38	26%	1,570	124	9.3
Epsilon	HFPS-Bag	29.6	2.8	59	521 ± 5	21.5 ± 0.4	0.9	<0.05	19	1.6	322	8%	2235	1,078	8.8
Background seawater															
T09C-01, 996 m	Niskin-CTD	4.5	7.78	53	40 ± 0.3	38 ± 1.0	<0.1	<0.05	37	1.6	25	4%	69	<0.1	2.1
T09C-01, 1,598 m	Niskin-CTD	3.0	7.77	53	38 ± 07	39 ± 1.0	<0.1	<0.05	37	2.9	13	7%	100	<0.1	2.1
V09C-02, 1,557 m	Niskin-CTD	3.2	7.76	53	38 ± 0.4	39 ± 0.7	<0.1	<0.05	37	2.5	16	6%	103	<0.1	2.1

Note. Temperature not measured during sampling; or no aliquot was available for nitrate analysis and thus dissolved organic nitrogen could not be calculated. Abbreviation: N.A., not available.

4. Discussions

4.1. Sample Overview

The end-member of a high-temperature focused vent is typically obtained using Mg contents to correct seawater entrainment during seafloor sampling (Bischoff & Seyfried, 1978; Mottl, 1983; Seyfried et al., 2003). However, there is no suitable proxy to derive end-member of diffuse vents (Butterfield et al., 2011; Gamo et al., 1997). Nevertheless, the high temperatures (13–50°C), low pH (1.5–5.8), high silicate (>1,000 μM), high dissolved iron (21–1,078 μM) were all indicative of vigorous water-rock reactions. The fluids were likely to have been minimally mixed with seawater. Thus, the measured values without further correction were reported as the end-member values and discussed.

Table 3
Concentrations and Isotopic Compositions of Particulate Organic Carbon (POC) and Particulate Nitrogen (PN) for Suspended Particles in Hydrothermal Fluids from Three Diffuse Vents

Sample name	POC (μmol/L)	PN (μmol/L)	C/N-POM	δ^{13}C-POC (‰)	δ^{15}N-PN (‰)	Cell/L (±95% C.I.)	Dive #
Background seawater	0.23	0.028	8.1	−23.3	N.D.	2.5(±0.2)×104	CTD
Diffusive vent							
Creamsicle	–	–	–	–	–	1.3(±0.1)×105	J2-418
Red Rock	2.45	0.398	6.1	−15.5	N.D.	–	J2-418
Kohu	0.48	0.042	11.4	N.D.	N.D.	1.3(±0.2)×105	J2-414
Shrimp City	–	–	–	–	–	2.4(±0.3)×105	J2-414
Luo	3.08	0.605	5.1	−12.3	4.3	2.2(±0.2)×105	J2-417
Epsilon	–	–	–	–	–	2.2(±0.2)×105	J2-417

Notes. N.D.: Not detectable due to insufficient C and N materials collected for isotope analysis. The detection limit for POC is 8 μg and for PN is 2 μg. The isotopic compositions of carbon and nitrogen cannot be determined when POC and PN are lower than 10 and 8 μg, respectively.

Table 4
Concentrations of Dissolved Organic Carbon (DOC), Total Dissolved Nitrogen (TDN), Particulate Organic Carbon (POC), Particulate Nitrogen (PN), Turbidity (dNTU), and Oxidation and Reduction Potential (ORP) in the W

Station (cast ID)	Depth (m)	DOC (μM)	TDN (μM)	POC (μmol/L)	PN (μmol/L)	C/N-POM	$\delta^{13}C_{\text{-POC}}$ (‰)	Si (μM)	Fe (μM)	dNTU	ORP-02	ORP-07	Niskin bottle #	UH ID
Plume above W. Mata summit (1176m. 15.09°S, 173. 75°W; above active eruption sites)														
V09C01	1,092	45 ± 1.0	40 ± 0.8	0.28	0.031	8.8	−25.3	–	<0.1	0.003	−27	15	24	7
V09C01	1,096	45 ± 0.9	39 ± 0.3	0.46	0.044	10.5	−21.5	–	<0.1	1.459	−91	−141	16	6
V09C01	1,099	44 ± 0.1	39 ± 0.6	0.50	0.045	11.0	−22.4	78	<0.1	1.262	−82	−115	20	5
V09C01	1,134	45 ± 1.1	39 ± 0.8	0.56	0.050	11.2	−24.8	78	<0.1	0.062	53	102	45	4
Above Maka (1569m. 15.42°S, 174. 28°W)														
V09C02	1557	38 ± 0.4	39 ± 0.7	0.28	0.029	9.6	−22.1	–	–	0.045	26	137	17	34
V09C02	1297	41 ± 0.8	39 ± 0.7	–	–	–	–	91	<0.1	0.001	35	123	21	7
V09C02	1370	40 ± 2.0	39 ± 0.5	0.23	0.028	8.0	−24.4	90	<0.1	0.001	25	116	20	43
Background seawater (NELSC)														
T09C-01	996	40 ± 0.3	38 ± 1.0	0.14	0.015	9.1	–	69	<0.1	0.001	32	230	18	16
T09C-01	1,598	38 ± 0.7	39 ± 1.0	0.23	0.028	8.1	−23.3	82	<0.1	0.004	130	226	52	15

Notes. Mata vent sites. Seawater samples were collected with Niskin bottles on a CTD rosette deployed from the research vessel.

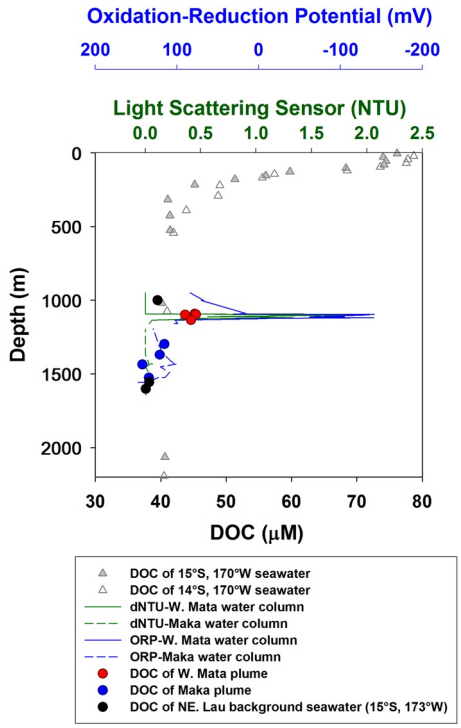

Figure 3. Dissolved organic carbon (DOC) concentrations in hydrothermal plume fluids and background seawater. Filled circles are DOC data from this study. Open and filled triangles are DOC data generated and published on-line by Dennis Hansell at the University of Miami to provide additional local background seawater values (15°S, 170°W; 14°S, 170°W, transect P15S of WOCE/CLIVAR http://yyy.rsmas.miami.edu/groups/biogeochem/Data.html).

4.2. Biological Production of Organic Carbon

4.2.1. Carbon-Fixation Pathways

To explore the organic biogeochemistry of the W. Mata vent field in a global context, we summarized literature values of DOC, POC, $C/N_{\text{-POM}}$, and δ^{13}C-POC for various deep-sea hydrothermal vents and plumes in Table 5. Biological organic carbon production in the W. Mata back-arc spreading hydrothermal system is evidenced by the elevated DOC and POC, elevated cell abundances (Table 3), Redfield-like $C/N_{\text{-POM}}$, distinct δ^{13}C-POC values, and the depleted TDN. Additional evidence comes from the abundant filamentous microbial mats observed at Epsilon and Creamsicle (Figure 2). Scattered microbial mats were also observed at Shrimp City and Luo, where high abundances of indigenous shrimp were also present (Figure 2).

The cell abundances (1.3×10^5 to 2.4×10^5 cells/mL) within the diffuse vent fluids were 5-to-10 folds higher than those in background seawater ($2.5 \pm 0.2 \times 10^4$ cells/mL). The high cell counts were consistent with elevated POC and PN concentrations (Table 3). The POC in the Red Rock Ridge and Luo vent fluids had C/N ratios similar to the Redfield ratio (6.6), indicating that the POC was freshly made biomass. The C/N of POC from Kohu vent is much higher than those from the Red Rock and Luo vents, suggesting that the POC from Kohu might have undergone some degree of degradation (Table 3). Degradation of POC preferentially removes N over C, resulting in elevated C/N ratios (Martin et al., 1987). Alternatively, the production of carbon-rich POM such as polysaccharides.

The POC in Red Rock and Luo vents were significantly more enriched in ^{13}C than that in nearby background seawater (−23 ± 1‰, Table 3) or in the hydrothermal-vent-influenced sinking particles from the Tonga arc region (−24.3‰ to −21.4‰; Kim et al., 2016) (Table 5). The majority of the W. Mata POC must have been produced within the subsurface or on the seafloor, and only to a small extent accumulated sinking particles

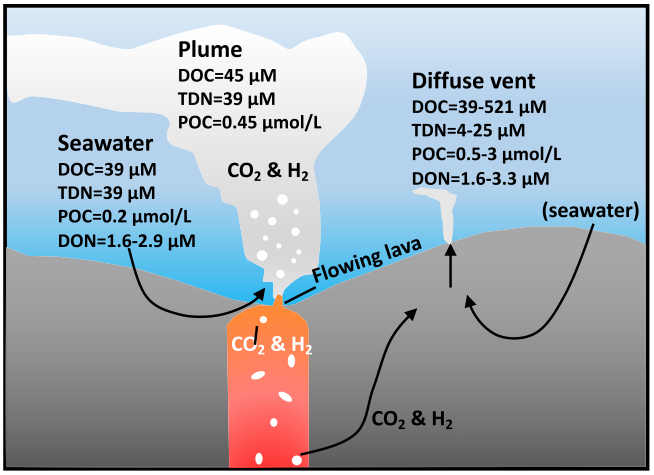

Figure 4. Schematic drawing of the production of organic carbon (DOC) and depletion of total dissolved nitrogen (TDN) in West Mata vent field. In this model, high DOC is produced within the subsurface and at the seafloor or on the vent surface habitats. The circulating hydrothermal fluids entrain DOC before and after the fluids are heated. Some DOC may be generated by thermal degradation of particulate organic carbon during the ascending of hydrothermal fluids, resulting in high DOC observed in fluids collected. Drawing modified from Butterfield et al. (2011). POC, particulate organic carbon. DON, dissolved organic nitrogen.

such as the POC from the water column (Table 3). The ^{13}C enrichment suggests that the resident vent biomes fixed carbon via a pathway with small carbon isotope fractionation (ε) between bicarbonate and POC. From dissolved inorganic carbon (DIC) in a typical hydrothermal vent with a $\delta^{13}C$-DIC value between 0‰ to −9‰ (Takai et al., 2008; Walker et al., 2008; Zerkle et al., 2005), vent biome would generate organic carbon with $\delta^{13}C$-POC values of −0.2‰ to −14.5‰ via the reductive tricarboxylic acid (rTCA) cycle (ε of 2–5.5‰) or via the 3-hydroxypropionate/4-hydroxybutyrate (3-HP/4-HB) cycle (ε of 0.2–3.6‰) (House et al., 2003; Zerkle et al., 2005; Zhang et al., 2002). In contrast, the biomass would have $\delta^{13}C_{\text{-POC}}$ values of between −22‰ and −44.5‰ via the Calvin-Benson cycle (ε of 22–35.5‰) (e.g., Wong & Sackett, 1978).

The use of the rTCA cycle for biomass synthesis requires much less energy than the Calvin-Benson cycle (White et al., 2012). Thus, chemolithotrophic micro-organisms residing in hydrothermal environments may have adapted to utilize such metabolic pathways to thrive in places where available energy is constrained by the total amounts of available chemical compounds (McCollom & Amend, 2005). Based on genomic sequences, rTCA cycles have been suggested to be the carbon fixation pathways for some deep-sea hydrothermal isolates or closely related strains (Hügler & Sievert, 2011), for example, *phylum Aquificae* (Hügler et al., 2007), *Epsilonproteobacteria* (Hügler et al., 2005), and *thermophilic archaeon Pyrococcus sp. Strain NA2* (Lee et al., 2011). Organisms utilizing the 3-HP cycle are not yet isolated but have been suggested to be important contributors at deep-sea hydrothermal vents (Nakagawa & Takai, 2008; Nakagawa et al., 2006).

4.2.2. Enhanced Nitrogen Fixation and Denitrification

The TDN concentrations in the West Mata low-temperature diffuse vents were much lower than those in bottom seawater (Table 2), indicating available nitrogen was consumed likely by organisms in a prosperous subseafloor and surface vent habitat. Similar to photosynthesis, chemosynthesis converts DIC, and dissolved inorganic nitrogen (DIN) into POM (Gruber, 2008). In an anoxic environment, denitrifiers reduce nitrate, ultimately into nitrogen gas, decreasing the nitrate concentration in the fluids (Bourbonnais et al., 2012; Butterfield et al., 2004; Devol, 2008). All of the surveyed W. Mata low-temperature diffuse vents contained ammonium, demonstrates nitrate reduction along the fluid flow paths.

The dissolved and particulate nitrogen was not mass-balanced between the recharging background seawater and the discharging diffuse vents. The total decrease in the TDN was 14 and 25 μM, exceeding the combined increase in PN and DON in the Red Rock and Luo vents (1.87 and 2.28 μmol/L) (Tables 2 and 4). The PN only measured the suspended organic matter (living cells and detritus) in the vent fluids retained on the filters. In contrast, the DON measures the organic nitrogen dissolved in the water. The rest of the lost TDN was likely converted into rock-attached biomass and biofilms within the subsurface. Alternatively, denitrification ultimately to gaseous nitrogen within the subsurface was a dominant process.

The sources and sinks of the DON in the hydrothermal system are intimately linked to assimilation, nitrification, and denitrification. Microbial, macrofauna, and microfauna activities on the seafloor and the subsurface release the DON into the hydrothermal fluids. Heterotrophic activities consume DON, and heat degradation reduces DON in the hydrothermal systems. These DON input and removal processes might alter the $C/N_{\text{-DOM}}$. The Creamsicle, Red Rock, and Kohu vents had $C/N_{\text{-DOM}}$ ranged from 14 to 25, similar to the $C/N_{\text{-DOM}}$ of nearby background seawater (13–25; Table 2). The high $C/N_{\text{-DOM}}$ in Shirmp City (40) and Luo (38) suggests that the vent-derived DOM might contain more aromatic compounds than the DOM from other vent sites. Shrimps were abundant in Shirmp City (40) and Luo (Figure 2), suggesting possible DOM derived from the shrimp-ectosymbionts and from the metacommunity activities (Zbinden & Cambon-Bonavita, 2020). The elevated $C/N_{\text{-DOM}}$ over the $C/N_{\text{-POM}}$ (6.1–11.2) observed for the Red Rock, Kohu, and Luo vents suggests preferential removal of N-containing organic matter during the transformation from

Table 5
Summary of Dissolved Organic Carbon (DOC), Particulate Organic Carbon (POC) Concentrations, δ^{13}C-POC (‰), and The C to N Ratio of The Particulate Organic Matter ($C/N_{\text{-POM}}$) of This Research and in The Literature

Study sites	DOC (μM)	POC (μmol/L)	δ^{13}C-POC (‰)	$C/N_{\text{-POM}}$	Reference
Background seawater					
West Mata, Lau (956 m &1,598 m)	38–40	0.14–0.23	−23	8–9	This study
North Central Pacific (Eve 1; 1,800–5,600 m)	34–38	0.049–0.129	−21.7 to −22.6	–	Druffel et al. (1992)
Sargasso Sea (Hydro 6; 852–4,450 m)	40–43	0.040–0.106	−20.2 to −20.5	–	Druffel et al. (1992)
East Pacific Rise 9°50′N	37–39	0.11–0.21	–	–	Bennet, Statham, et al. (2011)
East Pacific Rise 21°N	–	–	–	24	Comita et al. (1984)
Loihi (1,003 m & 1,072 m)	39.2–40.4	0.1	–	–	Bennet, Hansman, et al. (2011)
North Pond (4,000 m)	40–50	0.1–0.3	–	7–8	Meyer et al. (2016); Walter et al. (2018)
Hydrothermal plume					
Above West Mata vent field	44–45	0.28–0.56	−21.5 to −25.3	9–11	This study
Loihi sea mount; dispersing plume	41–60	0.06–0.2	−20 to −28	–	Bennet, Hansman, et al. (2011)
East Pacific Rise 9°50′N	35–43	0.07–0.46	–	–	Bennet, Statham, et al. (2011)
East Pacific Rise 9°50′N; near-field buoyant plume	38–39	0.87–3.81	–	–	Bennet, Statham, et al. (2011)
Low-temperature diffuse vent					
West Mata, Lau	39–521	2.5–4.1	−12.3 to −15.5	5–11	This study
Baby Bare, Juan de Fuca	7–27	–	–	–	Lang et al. (2006)
Endeavor	42–69	–	–	–	Lang et al. (2006)
Axial Volcano	34–71	–	–	–	Lang et al. (2006)
Axial Volcano	61–189	–	–	–	Hawkes et al. (2015),[b]
Loihi sea mount	54–92	–	–	–	Bennet, Hansman, et al. (2011)
East Pacific Rise 9°50′N; near field vent	38–47	0.87–3.81	–	–	Bennet, Statham, et al. (2011)
East Pacific Rise 21°N	–	0.4-1[a]	–	12–18	Comita et al. (1984)
High-temperature focused vent					
Lost City	101–106	–	–	–	Lang et al. (2010)
Endeavor	11–26	–	–	–	Lang et al. (2006)
Endeavor	15–22	–	–	–	Hawkes et al. (2015),[b]
Axial Volcano	8–24	–	–	–	Lang et al. (2006)
Axial Volcano	24–50	–	–	–	Hawkes et al. (2015),[b]
Izena, Okinawa Trough	–	5.8–9.2	–	–	Myruyama et al. (1993)
Ridge flank crustal fluids					
Juan de Fuca	9–17	0.05–0.09	−34	–	Lin et al. (2019)
North Pond	18–43	0.4–1.2	–	27–62	Meyer et al. (2016); Walter et al. (2018)

	Porewater DOC (μM)	POC (%)	δ^{13}C-POC (‰)	Reference
Porewater from vent microbial mats				
Loihi sea mount	68–179	0.28–0.63	−23 to −26	Bennet, Hansman, et al. (2011)
Hydrothermal-influenced sinking particles				
Tonga arc	–	>0.7–6	−23 to −24.3	Kim et al. (2016)

Note. Dashes indicate that samples were not measured for the particular component.
[a]Comita et al. (1984) reported a factor of 2–5 times more elevated than the non-vent fluid without providing the quantified values. We calculated by assuming a background non-vent fluid at the 21°N same as the 9°50′N by Bennet, Statham, et al. (2011). [b]Only the samples collected with HFPS bags were summarized. Readers are encouraged to see additional DOC data in Hawkes et al. (2015).

POM to DOM. The relatively low $C/N_{\text{-DOM}}$ (14) of the Red Rock sample corresponds well with the low $C/N_{\text{-POM}}$ (6.1).

The very high DOC in the Epsilon fluid sample may seem suspicious but is not exceptional because Hawkes et al. (2015) reported high DOC concentrations in various vent fields. Large filamentous microbial mats were observed at Epsilon (Figure 2f). The filamentous bacterial microbial mat matrix often consists of carbon-rich polysaccharides (Elshahed et al., 2003; Emerson et al., 2007; Moyer et al., 1995). The solubility of microbial mats may leach DOM with high C/N. The measured dissolved hydrogen concentration was too low (58 μmol/Kg, Baumberger et al., 2014) to permit spontaneous abiotic formic acid production from H_2 and CO_2 (Supporting information, Figure S1, Tables S1 and S2). The abiotic formic acid reaction becomes thermodynamically favorable (exergonic, negative Gibbs free energy) when the environment contains a much higher H_2 concentration (up to 30 mmol/Kg) (Figure S1). Therefore, the high DOC at Epsilon cannot be explained by abiotic formic acid production as those observed in the Von Damm vent field (Lang et al., 2010).

4.3. Impact on the Water Column

Within the particle-rich neutrally buoyant plume above the W. Mata vent field, POC and PN concentrations are twice those of the background seawater values (Table 4). Because there is no significant increase in Si concentrations in the plume samples relative to background seawater samples, we estimate a minimum of a hundred-time dilution in forming the plume from the volcanic activities and the diffuse vents. Such a dilution factor agrees with typical three-to-five orders of magnitude dilution of the source hydrothermal vent fluids observed elsewhere (e.g., Cowen et al., 2003; Edmonds et al., 2003; Field & Sherrell, 2000; Lupton et al., 1985). Using a dilution factor of a hundred, we estimated that a maximum of 0.03 μmol-C/L of POC could have been injected from the diffuse vent fluids with high POC (e.g., Red Rock Ridge and Luo). Although we did not collect fluid samples for POC analysis from sites adjacent to molten lava, we can assume that POC could not escape from the high-temperature molten lava. Accordingly, the POC from diffuse vents accounts for no more than 13% of the averaged increase in POC (0.23 μmol-C/L) in the plume sample. Therefore, most of the elevated POC in the plume samples was likely produced within the plume as a result of enhanced biological activities induced by the elevated supply of reducing species—including dissolved iron, hydrogen sulfide, hydrogen, and ammonium—into the overlying water column as indicated by the anomaly in ORP (Table 4).

Earlier thermodynamic calculations (McCollom, 2000) predicted that the potential primary productivity by oxidizing the amount of reducing species in mid-ocean-ridge black smoker derived hydrothermal plume is up to 50 mg dry weight biomass/L-vent fluid, which is approximately 1.9 mmol-C/L recalculated based on biomass to carbon conversion factor of 0.46 and a carbon molar mass of twelve (Battley, 1998). Our measured POC content (0.45 ± 0.12 μmol-C/L) in the plume is three orders of magnitude lower than that predicted by McCollom (2000). We attribute the low POC to the much lower sulfur, sulfide, and hydrogen concentrations measured in the W. Mata plume samples than the estimated concentrations used for McCollom (2000) model. Hence, we recalculated the potential "dark" carbon production based on the maximum measured concentrations of dissolved hydrogen (14,843 nM), total dissolved iron (6,180 nM), total manganese (359 nM), and elemental sulfur (61,646 nM) in the 2008 plum (Table 6) (Resing et al., 2011). For easy comparison, we directly applied the ΔG^0 reported in McCollom (2000) because of the differences in values of ΔG^0 due to the changes in pressure—120 bar at W. Mata versus 250 bar in the mid-ocean-ridge black smoker—is minimum. Our modeled results (Table 7) show that the reducing species in the 2008 plume can potentially support at least 4.2 μmol-C/L primary carbon production or 0.11 mg-dry wet per kilogram of plume water. The thermodynamically estimated primary carbon production is similar to the combined increase in DOC and POC (4.5 μmol-C/L) observed in the 2009 plume. Our result demonstrates that chemoautotrophs were quite effective in utilizing available reducing compounds to producing organic carbon.

The DOC increase (~4 μM) was 11 times higher than the POC increase in the W. Mata plume than background seawater values. In comparison, there was an approximate 10–20 μM DOC increase without a significant POC increase within the Loihi plume (Bennett, Hansman, et al., 2011) (Table 5). In

Table 6
Estimated Chemical Compositions and Activities of W. Mata Plume Used for Thermodynamic Modeling

Chemical species	Unit	Value	Activity coefficient	Activity	log(activity)	Sources
SO_4^{2-}	mM	28	0.2	5.6E-03	−2.3	Average seawater value
$O_{2(aq)}$	μM	150	1	1.5E-04	−3.8	From WOCE P15
$H_{2(aq)}$	nM	14,843	1	1.5E-05	−4.8	Resing et al. (2011); Table S1
Fe^{2+}	nM	6,180	0.2	1.2E-06	−5.9	Estimated from the highest PFe = 4,120 nM, and dissolve Fe = 1.5 × PFe and assuming all dissolved Fe is Fe^{2+} in Resing et al. (2011); Table S1
Mn^{2+}	nM	359	0.2	7.2E-08	−7.1	Assuming all TMn is Mn^{2+} in Resing et al. (2011); Table S1
$S^0_{(s)}$	nM	41,646	–	–	–	Resing et al. (2011); Table S1
HCO_3^-	μM	2640	0.55	1.5E-03	−2.8	Resing et al. (2011); Table S1

Note. Mata plume used for thermodynamic modeling.

contrast, a maximum POC increase of 0.2 μmol/L was observed with a DOC decrease of 2 μM in the 9°15′N East Pacific Rise plumes, which the authors explained as adsorption of DOC by the rich particles in the plume to form POC and heterotrophic biological consumption of DOC (Bennett, Statham, et al., 2011). Further research is needed to unravel mechanisms, such as aging of a hydrothermal plume and microbial community structures, regulating the production and consumption of organic carbon, resulting in the different partitioning between the chemolithoautotrophic DOC and POC among various plumes.

5. Conclusion and Future Research Directions

The DOC, TDN, NO_3^-, NH_4^+, DON, and POC distribution in the West Mata eruptive vent field was summarized with a schematic drawing (Figure 4). The elevated DOC in the low-temperature diffuse vents is explained by biological production. Elevated POC and cell counts and depleted TDN support vigorous biological production within the subseafloor and seafloor habitats associated with diffuse vents. The low $C/N_{\text{-POM}}$

Table 7
Thermodynamic Calculation of Potential Metabolic Energy Available for A Few Selected Chemolithoautotrophic Reactions Occurring in the West Mata Hydrothermal Plume

Chemolithoautotrophic energy source	Overall reaction	ΔG^0 (Kcal)	lnQ	ΔG (Kcal/mol reactant)	Limiting reactant	Limiting reactant concentration (M)[a]	Available energy (cal/kg plume fluid)[b]	Primary biomass potential (mg dry wt/kg plume)[c]	Organic carbon production (μmol-C/kg plume)[d]
Iron (II) oxidation	$Fe^{2+}+1/4O_{2(aq)}+2.5H_2O = Fe(OH)^-_3+2H^+$	−92	−32	−110	Fe^{2+}	6.2E-06	0.61	0.017	0.64
Mn (II) oxidation	$Mn^{2+}+1/2O_{2(aq)}+H_2O=MnO_{2(s)}+2H^+$	−1.8	−11	−8	Mn^{2+}	3.6E-07	0.003	0.00007	0.0026
Hydrogen oxidation	$H_{2(aq)}+1/2O_{2(aq)} = H_2O$	−63	16	−55	$H_{2(aq)}$	1.5E-05	0.73	0.08025	3.07
Sulfur oxidation	$S_{0(s)}+3/2O_{2(aq)}+H_2O=SO_4^{2-}+2H^+$	−129	8	−124	$S^0_{(s)}$	4.2E-06	0.47	0.013	0.49
							Sum	0.11	4.2

Note. Primary biomass potential is also calculated. Parameters used for the calculation are listed in Table 6.
[a]Limiting reactant concentrations are derived from the measured concentrations in the 2008 plume reported by Resing et al. (2011). [b]Assuming 90% of the limiting reactant can be utilized. [c]Energy to biomass conversion factor is ~9,100 cal/g for hydrogen oxidizers and ~36,400 cal/g for other microbes (McCollom, 2000). [d]Biomass to organic carbon conversion factor = 0.46 (Battley, 1998).

in diffuse vent fluids further indicates freshly produced biomass. The DON concentrations in the diffuse vent fluids were similar to or slightly higher than those in recharging seawater. The higher $C/N_{\cdot DOM}$ than $C/N_{\cdot POM}$ supports preferential nitrogen removal during DOM formation. The ^{13}C-enriched POC implies that resident organisms along the fluid flow paths utilized carbon-fixation pathways different from marine phytoplankton.

The potential primary organic carbon production estimated from the energy derived through the oxidation of hydrothermally discharged reducing species into the water column matches the elevated organic carbon concentrations relative to background seawater values. Overall, this study confirms enhanced production of organic matter at northeast Lau hydrothermal vent fields and that unsedimented oceanic crust associated with back-arc spreading volcanism is a net DOC and POC source for the deep ocean.

Future research should include DOC characterization at the molecular level. Large volume—up to several tens of liters—fluid samples are needed for functional group analysis by nuclear magnetic resonance spectroscopy, molecular composition analysis by electrospray ionization (ESI) coupled with a Fourier-transform ion-cyclotron-resonance mass-spectrometry (FT-ICR MS) or with an Orbitrap Fusion™ Tribrid™ Mass Spectrometer. The stable and radiocarbon isotopic composition analysis can be performed by accelerator mass spectrometry (AMS). Large-volume-fluid samplers are available for collecting samples at low-temperature sites (e.g., Cowen et al., 2012; Lin et al., 2020; McCarthy et al., 2010). There is a need to develop a large-volume-fluid sampler that is not only DOC-contamination-free but also allows the collection of extremely high temperature and high gas content fluids near molten lava and high-temperature vents.

Data Availability Statement

The raw data are archived at BCO-DMO (https://www.bco-dmo.org/project/836899).

Acknowledgments
The authors thank the remotely operated-vehicle Jason II and research vessel Thomas Thompson crews for their skillful support during the field sampling. The authors also thank Chih-Chiang Hsieh, Natalie Hamada, and Kathryn Hu for their fantastic lab support. This project was supported by N.S.F. (OCE0929881, J. P. Cowen and K. H. Rubin), the NOAA PMEL VENTS (now Earth-Ocean Interactions) Program and the Joint Institute for the Study of the Atmosphere and Ocean (JISAO) under NOAA Cooperative Agreement No. NA10OAR4320148, and the UH NASA Astrobiology Institute. The Ministry of Science and Technology of Taiwan award (MOST 107-2611-M-002-002, and MOST 108-2611-M-002-006 to H.-T. Lin). Ministry of Education (M.O.E.) Republic of China (Taiwan) 109L892601 to H.-T. Lin. SOEST contributions no. 11285, C-DEBI contribution no. 563. PMEL contribution no. 3996, JISAO contribution 2183. There are no real or perceived conflicts of interest for any author.

References

Aristegui, J., Duarte, C. M., Agustı, S., Doval, M., Álvarez-Salgado, X. A., Hansell, D. A. (2002). Dissolved organic carbon support of respiration in the dark ocean. *Science*, *298*, 1967.

Azam, F., Fenchel, T., Field, J., Gray, J., Meyer-Reil, L., & Thingstad, F. (1983). The ecological role of water-column microbes in the sea. *Marine Ecology Progress Series*, *10*, 257–263. https://doi.org/10.3354/meps010257

Baker, E. T., Lupton, J. E., Resing, J. A., Baumberger, T., Lilley, M. D., Walker, S. L., & Rubin, K. H. (2011). Unique event plumes from a 2008 eruption on the Northeast Lau Spreading Center. *Geochemistry, Geophysics, Geosystems*, *12*, Q0AF02. https://doi.org/10.1029/2011gc003725

Baker, E. T., & Massoth, G. J. (1987). Characteristics of hydrothermal plumes from two vent fields on the Juan de Fuca Ridge, northeast Pacific Ocean. *Earth and Planetary Science Letters*, *85*, 59–73. https://doi.org/10.1016/0012-821x(87)90021-5

Battley, E. H. (1998). The development of direct and indirect methods for the study of the thermodynamics of microbial growth. *Thermochimica Acta*, *309*, 17–37. https://doi.org/10.1016/s0040-6031(97)00357-2

Baumberger, T., Lilley, M. D., Resing, J. A., Lupton, J. E., Baker, E. T., Butterfield, D. A., et al. (2014). Understanding a submarine eruption through time series hydrothermal plume sampling of dissolved and particulate constituents: West Mata, 2008–2012. *Geochemistry, Geophysics, Geosystems*, *15*, 4631–4650. https://doi.org/10.1002/2014GC005460

Bennett, S. A., Hansman, R. L., Sessions, A. L., Nakamura, K.-i., & Edwards, K. J. (2011). Tracing iron-fueled microbial carbon production within the hydrothermal plume at the Loihi seamount. *Geochimica et Cosmochimica Acta*, *75*, 5526–5539. https://doi.org/10.1016/j.gca.2011.06.039

Bennett, S. A., Statham, P. J., Green, D. R. H., Le Bris, N., McDermott, J. M., Prado, F., et al. (2011). Dissolved and particulate organic carbon in hydrothermal plumes from the East Pacific Rise, 9°50′N. *Deep Sea Research Part I: Oceanographic Research Papers*, *58*, 922–931. https://doi.org/10.1016/j.dsr.2011.06.010

Bischoff, J. L., & Seyfried, W. E. (1978). Hydrothermal chemistry of seawater from 25 degrees to 350 degrees C. *American Journal of Science*, *278*, 838–860. https://doi.org/10.2475/ajs.278.6.838

Bourbonnais, A., Lehmann, M. F., Butterfield, D. A., & Juniper, S. K. (2012). Subseafloor nitrogen transformations in diffuse hydrothermal vent fluids of the Juan de Fuca Ridge evidenced by the isotopic composition of nitrate and ammonium. *Geochemistry, Geophysics, Geosystems*, *13*(Q02T01), 1–23. https://doi.org/10.1029/2011gc003863

Bronk, D. A., Killberg-Thoreson, L., Sipler, R. E., Mulholland, M. R., Roberts, Q. N., Bernhardt, P. W., et al. (2014). Nitrogen uptake and regeneration (ammonium regeneration, nitrification and photoproduction) in waters of the West Florida Shelf prone to blooms of Karenia brevis. *Harmful Algae*, *38*, 50–62. https://doi.org/10.1016/j.hal.2014.04.007

Bronk, D., See, J., Bradley, P., & Killberg, L. (2007). DON as a source of bioavailable nitrogen for phytoplankton. *Biogeosciences*, *4*, 283–296. Retrieved from https://bg.copernicus.org/articles/4/283/2007/

Butterfield, D. A., Roe, K. K., Lilley, M. D., Huber, J. A., Baross, J. A., Embley, R. W., & Massoth, G. J. (2004). Mixing, reaction and microbial activity in the sub-seafloor revealed by temporal and spatial variation in diffuse flow vents at Axial Volcano. *Geophysical monograph*, *144*, 269–289. https://doi.org/10.1029/144gm17

Carlson, C. A. (2002). Production and removal processes. In D. A. Hansell, & C. A. Carlson (Eds.), *Biogeochemistry of marine dissolved organic matter* (pp. 91–151). Elsevier.

Carlson, C. A., & Hansell, D. A. (2015). DOM sources, sinks, reactivity, and budgets. In D. A. Hansell & C. A. (Eds.), *Carlson Biogeochemistry of marine dissolved organic matter* (pp. 65–126). Elsevier. ISBN 978-0-12-405940-5.

Carlson, C. A., Hansell, D. A., Peltzer, E. T., & Smith, W. O., Jr. (2000). Stocks and dynamics of dissolved and particulate organic matter in the southern Ross Sea, Antarctica. *Deep Sea Research Part II: Topical Studies in Oceanography*, *47*, 3201–3225. https://doi.org/10.1016/s0967-0645(00)00065-5

Cauwet, G., Miller, A., Brasse, S., Fengler, G., Mantoura, R. F. C., & Spitzy, A. (1997). Dissolved and particulate organic carbon in the western Mediterranean Sea. *Deep Sea Research Part II: Topical Studies in Oceanography*, *44*, 769–779. https://doi.org/10.1016/s0967-0645(96)00085-9

Clague, D. A., Paduan, J. B., Caress, D. W., Thomas, H., Chadwick, W. W., & Merle, S. G. (2011). Volcanic morphology of West Mata Volcano, NE Lau Basin, based on high-resolution bathymetry and depth changes. *Geochemistry, Geophysics, Geosystems*, *12*. https://doi.org/10.1029/2011gc003791

Comita, P. B., Gagosian, R. B., & Williams, P. M. (1984). Suspended particulate organic material from hydrothermal vent waters at 21° N. *Nature*, *307*, 450–453. https://doi.org/10.1038/307450a0

Cowen, J. P., Copson, D. A., Jolly, J., Hsieh, C.-C., Lin, H.-T., Glazer, B. T., & Wheat, C. G. (2012). Advanced instrument system for real-time and time-series microbial geochemical sampling of the deep (basaltic) crustal biosphere. *Deep Sea Research Part I: Oceanographic Research Papers*, *61*, 43–56. https://doi.org/10.1016/j.dsr.2011.11.004

Cowen, J. P., Giovannoni, S. J., Kenig, F., Johnson, H. P., Butterfield, D., Rappe, M. S., et al. (2003). Fluids from aging ocean crust that support microbial life. *Science*, *299*, 120–123. https://doi.org/10.1126/science.1075653

Devol, A. (2008). Denitrification including anammox. In D. Capone, D. Bronk, M. Mulholland, & E. Carpenter (Eds.), *Nitrogen in the marine environment* (2nd ed., pp. 263–301). Amsterdam: Elsevier.

Druffel, E. R. M., Williams, P. M., Bauer, J. E., & Ertel, J. R. (1992). Cycling of dissolved and particulate organic matter in the open ocean. *Journal of Geophysical Research*, *97*, 15639–15659. https://doi.org/10.1029/92jc01511

Ducklow, H. W., & Carlson, C. A. (1992). Oceanic bacterial production. *Advances in Microbial Ecology*, *12*, 113–181. https://doi.org/10.1007/978-1-4684-7609-5_3

Edmonds, H. N., Michael, P. J., Baker, E. T., Connelly, D. P., Snow, J. E., Langmuir, C. H., et al. (2003). Discovery of abundant hydrothermal venting on the ultraslow-spreading Gakkel ridge in the Arctic Ocean. *Nature*, *421*, 252–256. https://doi.org/10.1038/nature01351

Elshahed, M. S., Senko, J. M., Najar, F. Z., Kenton, S. M., Roe, B. A., Dewers, T. A., et al. (2003). Bacterial diversity and sulfur cycling in a mesophilic sulfide-rich spring. *Applied and Environmental Microbiology*, *69*, 5609–5621. https://doi.org/10.1128/aem.69.9.5609-5621.2003

Embley, R. W., Merle, S. G., Baker, E. T., Rubin, K. H., Lupton, J. E., Resing, J. A., et al. (2014). Eruptive modes and hiatus of volcanism at West Mata seamount, NE Lau basin: 1996–2012. *Geochemistry, Geophysics, Geosystems*, *15*, 4093–4115. https://doi.org/10.1002/2014GC005387

Emerson, D., Rentz, J. A., Lilburn, T. G., Davis, R. E., Aldrich, H., Chan, C., & Moyer, C. L. (2007). A novel lineage of proteobacteria involved in formation of marine Fe-oxidizing microbial mat communities. *PLoS One*, *2*, e667. https://doi.org/10.1371/journal.pone.0000667

Engel, A., Harlay, J., Piontek, J., & Chou, L. (2012). Contribution of combined carbohydrates to dissolved and particulate organic carbon after the spring bloom in the northern Bay of Biscay (North-Eastern Atlantic Ocean). *Continental Shelf Research*, *45*, 42–53. https://doi.org/10.1016/j.csr.2012.05.016

Field, M. P., & Sherrell, R. M. (2000). Dissolved and particulate Fe in a hydrothermal plume at 9°45′N, East Pacific Rise. *Geochimica et Cosmochimica Acta*, *64*, 619–628. https://doi.org/10.1016/s0016-7037(99)00333-6

Fukuda, R., Ogawa, H., Nagata, T., & Koike, I. (1998). Direct determination of carbon and nitrogen contents of natural bacterial assemblages in marine environments. *Applied and Environmental Microbiology*, *64*, 3352–3358. https://doi.org/10.1128/aem.64.9.3352-3358.1998

Gamo, T., Okamura, K., Charlou, J-L., Urabe, T., Auzende, J.-M., Ishibashi, J., et al. (1997). Acidic and sulfate-rich hydrothermal fluids from the Manus back-arc basin, Papua New Guinea. *Geology*, *25*, 139–142.

German, C. R., Baker, E. T., Connelly, D. P., Lupton, J. E., Resing, J., Prien, R. D., et al. (2006). Hydrothermal exploration of the Fonualei Rift and spreading center and the Northeast Lau spreading center. *Geochemistry, Geophysics, Geosystems*, *7*, Q11022. https://doi.org/10.1029/2006gc001324

Gibbs, C. R. (1976). Characterization and application of ferrozine iron reagent as a ferrous iron indicator. *Analytical Chemistry*, *48*, 1197–1201. https://doi.org/10.1021/ac50002a034

Grasshoff, K., Kremling, K., & Ehrhardt, M. (1999). *Methods of seawater analysis*.

Griffith, D. R., McNichol, A. P., Xu, L., McLaughlin, F. A., Macdonald, R. W., Brown, K. A., & Eglinton, T. I. (2012). Carbon dynamics in the western Arctic Ocean: Insights from full-depth carbon isotope profiles of DIC, DOC, and POC. *Biogeosciences*, *9*, 1217–1224. https://doi.org/10.5194/bg-9-1217-2012

Gruber, N. (2008). The marine nitrogen cycle: Overview and challenges. In D. G. Capone, D. A. Bronk, M. R. Mulholland, & E. J. Carpenter (Eds.), *Nitrogen in the marine environment* (2nd ed., pp. 1–50). Burlington: Elsevier.

Hügler, M., Huber, H., Molyneaux, S. J., Vetriani, C., & Sievert, S. M. (2007). Autotrophic CO_2 fixation via the reductive tricarboxylic acid cycle in different lineages within the phylum Aquificae: Evidence for two ways of citrate cleavage. *Environmental Microbiology*, *9*, 81–92. https://doi.org/10.1111/j.1462-2920.2006.01118.x

Hügler, M., & Sievert, S. M. (2011). Beyond the Calvin cycle: Autotrophic carbon fixation in the ocean. *Annual Review of Marine Science*, *3*, 261–289. https://doi.org/10.1146/annurev-marine-120709-142712

Hügler, M., Wirsen, C. O., Fuchs, G., Taylor, C. D., & Sievert, S. M. (2005). Evidence for autotrophic CO_2 fixation via the reductive tricarboxylic acid cycle by members of the ε subdivision of proteobacteria. *Journal of Bacteriology*, *187*, 3020–3027.

Hansell, D., & Carlson, C. A. (2001). Marine dissolved organic matter and the carbon cycle. *Oceanography*, *14*, 41–49. https://doi.org/10.5670/oceanog.2001.05

Hansell, D., Carlson, C., Repeta, D., & Schlitzer, R. (2009). Dissolved organic matter in the ocean: A controversy stimulates new insights. *Oceanography*, *22*, 202–211. https://doi.org/10.5670/oceanog.2009.109

Hawkes, J. A., Rossel, P. E., Stubbins, A., Butterfield, D., Connelly, D. P., Achterberg, E. P., et al. (2015). Efficient removal of recalcitrant deep-ocean dissolved organic matter during hydrothermal circulation. *Nature Geoscience*, *8*, 856–860. https://doi.org/10.1038/ngeo2543

Hawkins, J. W. (1995). Evolution of the Lau Basin: Insights from ODP leg 135. In B. Taylor & J. Natland (Eds.), *Active margins and marginal basins of the Western Pacific* (Geophysical Monograph Series, 88, pp. 125–173). https://doi.org/10.1029/gm088p0125

Hayes, J. M. (2001). Fractionation of carbon and hydrogen isotopes in biosynthetic processes. *Reviews in Mineralogy and Geochemistry*, *43*, 225–277. https://doi.org/10.2138/gsrmg.43.1.225

Helgeson, H. C., Kirkham, D. H., & Flowers, G. C. (1981). Theoretical prediction of the thermodynamic behavior of aqueous electrolytes by high pressures and temperatures; IV, Calculation of activity coefficients, osmotic coefficients, and apparent molal and standard and relative partial molal properties to 600 degrees C and 5kb. *American Journal of Science*, *281*, 1249–1516. https://doi.org/10.2475/ajs.281.10.1249

Hofmann, M., Wolf-Gladrow, D. A., Takahashi, T., Sutherland, S. C., Six, K. D., & Maier-Reimer, E. (2000). Stable carbon isotope distribution of particulate organic matter in the ocean: A model study. *Marine Chemistry*, *72*, 131–150. https://doi.org/10.1016/s0304-4203(00)00078-5

Honjo, S., Manganini, S. J., Krishfield, R. A., & Francois, R. (2008). Particulate organic carbon fluxes to the ocean interior and factors controlling the biological pump: A synthesis of global sediment trap programs since 1983. *Progress in Oceanography*, *76*, 217–285. https://doi.org/10.1016/j.pocean.2007.11.003

House, C. H., Schopf, J. W., & Stetter, K. O. (2003). Carbon isotopic fractionation by Archaeans and other thermophilic prokaryotes. *Organic Geochemistry*, *34*, 345–356. https://doi.org/10.1016/s0146-6380(02)00237-1

Huber, J. A., Johnson, H. P., Butterfield, D. A., & Baross, J. A. (2006). Microbial life in ridge flank crustal fluids. *Environmental Microbiology*, *8*, 88–99. https://doi.org/10.1111/j.1462-2920.2005.00872.x

Jiao, N., Herndl, G. J., Hansell, D. A., Benner, R., Kattner, G., Wilhelm, S. W., et al. (2010). Microbial production of recalcitrant dissolved organic matter: Long-term carbon storage in the global ocean. *Nature Reviews Microbiology*, *8*, 593–599. https://doi.org/10.1038/nrmicro2386

Johnson, J. W., Oelkers, E. H., & Helgeson, H. C. (1992). SUPCRT92: A software package for calculating the standard molal thermodynamic properties of minerals, gases, aqueous species, and reactions from 1 to 5000 bar and 0 to 1000°C. *Computers & Geosciences*, *18*, 899–947. https://doi.org/10.1016/0098-3004(92)90029-q

Jones, R. D. (1991). An improved fluorescence method for the determination of nanomolar concentrations of ammonium in natural waters. *Limnology & Oceanography*, *36*, 814–819. https://doi.org/10.4319/lo.1991.36.4.0814

Kim, H. J., Kim, J., Pak, S. J., Ju, S.-J., Yoo, C. M., Kim, H. S., et al. (2016). Geochemical characteristics of sinking particles in the Tonga arc hydrothermal vent field, southwestern Pacific. *Deep Sea Research Part I: Oceanographic Research Papers*, *116*, 118–126. https://doi.org/10.1016/j.dsr.2016.07.015

Lang, S. Q., Butterfield, D. A., Lilley, M. D., Paul Johnson, H., & Hedges, J. I. (2006). Dissolved organic carbon in ridge-axis and ridge-flank hydrothermal systems. *Geochimica et Cosmochimica Acta*, *70*, 3830–3842. https://doi.org/10.1016/j.gca.2006.04.031

Lang, S. Q., Butterfield, D. A., Schulte, M., Kelley, D. S., & Lilley, M. D. (2010). Elevated concentrations of formate, acetate and dissolved organic carbon found at the Lost City hydrothermal field. *Geochimica et Cosmochimica Acta*, *74*, 941–952. https://doi.org/10.1016/j.gca.2009.10.045

Lee, H. S., Bae, S. S., Kim, M.-S., Kwon, K. K., Kang, S. G., & Lee, J.-H. (2011). Complete genome sequence of hyperthermophilic Pyrococcus sp. NA2 isolated from deep-sea hydrothermal vent area. *Journal of Bacteriology*, *193*, 3666–3667.

Lin, H.-T., Cowen, J. P., Olson, E. J., Amend, J. P., & Lilley, M. D. (2012). Inorganic chemistry, gas compositions and dissolved organic carbon in fluids from sedimented young basaltic crust on the Juan de Fuca Ridge flanks. *Geochimica et Cosmochimica Acta*, *85*, 213–227. https://doi.org/10.1016/j.gca.2012.02.017

Lin, H.-T., Cowen, J. P., Olson, E. J., Lilley, M. D., Jungbluth, S. P., Rappé, M. S., & Wilson, S. T. (2014). Dissolved hydrogen and methane in the oceanic basaltic biosphere. *Earth and Planetary Science Letters*, *405*, 62–73.

Lin, H.-T., Hsieh, C.-C., Repeta, D. J., & Rappé, M. S. (2020). Sampling of basement fluids via Circulation Obviation Retrofit Kits (CORKs) for dissolved gases, fluid fixation at the seafloor, and the characterization of organic carbon. *Methods X*, *7*, 101033.

Lin, H.-T., Repeta, D. J., Xu, L., & Rappé, M. S. (2019). Dissolved organic carbon in basalt-hosted deep subseafloor fluids of the Juan de Fuca Ridge flank. *Earth and Planetary Science Letters*, *513*, 156–165. https://doi.org/10.1016/j.epsl.2019.02.008

Longnecker, K., Sievert, S. M., Sylva, S. P., Seewald, J. S., & Kujawinski, E. B. (2018). Dissolved organic carbon compounds in deep-sea hydrothermal vent fluids from the East Pacific Rise at 9°50′N. *Organic Geochemistry*, *125*, 41–49. https://doi.org/10.1016/j.orggeochem.2018.08.004

Lupton, J. E., Delaney, J. R., Johnson, H. P., & Tivey, M. K. (1985). Entrainment and vertical transport of deep-ocean water by buoyant hydrothermal plumes. *Nature*, *316*, 621–623. https://doi.org/10.1038/316621a0

Martin, J. H., Knauer, G. A., Karl, D. M., & Broenkow, W. W. (1987). VERTEX: Carbon cycling in the northeast Pacific. *Deep Sea Research Part A. Oceanographic Research Papers*, *34*, 267–285. https://doi.org/10.1016/0198-0149(87)90086-0

Maruyama, A., Mita, N., & Higashihara, T. (1993). Particulate materials and microbial assemblages around the Izena black smoking vent in the Okinawa Trough. *Journal of Oceanography*, *49*, 353–367. https://doi.org/10.1007/bf02269570

McCarthy, M. D., Beaupré, S. R., Walker, B. D., Voparil, I., Guilderson, T. P., & Druffel, E. R. M. (2010). Chemosynthetic origin of 14C-depleted dissolved organic matter in a ridge-flank hydrothermal system. *Nature Geoscience*, *4*, 32–36. https://doi.org/10.1038/ngeo1015

McCollom, T. M. (2000). Geochemical constraints on primary productivity in submarine hydrothermal vent plumes. *Deep Sea Research Part I: Oceanographic Research Papers*, *47*, 85–101. https://doi.org/10.1016/s0967-0637(99)00048-5

McCollom, T. M., & Amend, J. P. (2005). A thermodynamic assessment of energy requirements for biomass synthesis by chemolithoautotrophic micro-organisms in oxic and anoxic environments. *Geobiology*, *3*, 135–144. https://doi.org/10.1111/j.1472-4669.2005.00045.x

McDermott, J. M., Seewald, J. S., German, C. R., & Sylva, S. P. (2015). Pathways for abiotic organic synthesis at submarine hydrothermal fields. *Proceedings of the National Academy of Sciences of the United States of America*, *112*, 7668–7672. https://doi.org/10.1073/pnas.1506295112

Meyer, J. L., Jaekel, U., Tully, B. J., Glazer, B. T., Wheat, C. G., Lin, H.-T., et al. (2016). A distinct and active bacterial community in cold oxygenated fluids circulating beneath the western flank of the Mid-Atlantic ridge. *Scientific Reports*, *6*, 1–14.

Mottl, M. J. (1983). Hydrothermal processes at seafloor spreading centers: Application of basalt-seawater experimental results. In P. A. Rona, K. Bostrom, L. Laubier, & K. L. J. Smith (Eds.), *Hydrothermal processes at seafloor spreading centers* (pp. 225–278). London, UK and New York, NY: Plenum Press.

Moyer, C. L., Dobbs, F. C., & Karl, D. M. (1995). Phylogenetic diversity of the bacterial community from a microbial mat at an active, hydrothermal vent system, Loihi Seamount, Hawaii. *Applied and Environmental Microbiology*, *61*, 1555–1562. https://doi.org/10.1128/aem.61.4.1555-1562.1995

Nakagawa, S., Inagaki, F., Suzuki, Y., Steinsbu, B. O., Lever, M. A., Takai, K., et al. (2006). Microbial community in black rust exposed to hot ridge flank crustal fluids. *Applied and Environmental Microbiology*, *72*, 6789–6799. https://doi.org/10.1128/aem.01238-06

Nakagawa, S., & Takai, K. (2008). Deep-sea vent chemoautotrophs: Diversity, biochemistry and ecological significance. *FEMS Microbiology Ecology*, *65*, 1–14. https://doi.org/10.1111/j.1574-6941.2008.00502.x

Popp, B. N., Laws, E. A., Bidigare, R. R., Dore, J. E., Hanson, K. L., & Wakeham, S. G. (1998). Effect of phytoplankton cell geometry on carbon isotopic fractionation. *Geochimica et Cosmochimica Acta*, *62*, 69–77. https://doi.org/10.1016/s0016-7037(97)00333-5

Preuss, A., Schauder, R., Fuchs, G., & Stichler, W. (1989). Carbon isotope fractionation by autotrophic bacteria with three different CO_2 fixation pathways. *Zeitschrift für Naturforschung*, *44*, 397–402.

Redfield, A. C. (1934). On the proportions of organic derivatives in sea water and their relation to the composition of plankton. *James Johnstone memorial volume*. (pp. 176–192). University Press of Liverpool.

Redfield, A. C. (1958). The biological control of chemical factors in the environment. *American Scientist*, *46*.

Repeta, D. J. (2015). Chemical characterization and cycling of dissolved organic matter. In D. Hansell, & C. Carlson (Eds.), *Biogeochemistry of marine dissolved organic matter* (pp. 21–63). https://doi.org/10.1016/b978-0-12-405940-5.00002-9

Resing, J. A., Rubin, K. H., Embley, R. W., Lupton, J. E., Baker, E. T., Dziak, R. P., et al. (2011). Active submarine eruption of boninite in the northeastern Lau Basin. *Nature Geoscience*, *4*, 799–806. https://doi.org/10.1038/ngeo1275

Rubin, K., Soule, S. A., Chadwick, W., Fornari, D., Clague, D., Embley, R., et al. (2012). Volcanic eruptions in the Deep Sea. *Oceanography*, *25*, 142–157. https://doi.org/10.5670/oceanog.2012.12

Schlitzer, R. (2000). Electronic atlas of WOCE hydrographic and tracer data now available. *Eos, Transactions, American Geophysical Union*, *81*, 45. https://doi.org/10.1029/00eo00028

Schlitzer, R., Anderson, R. F., Dodas, E. M., Lohan, M., Geibert, W., Tagliabue, A., et al. (2018). The GEOTRACES intermediate data product 2017. *Chemical Geology*, *493*, 210–223.

See, J. H., & Bronk, D. A. (2005). Changes in C:N ratios and chemical structures of estuarine humic substances during aging. *Marine Chemistry*, *97*, 334–346. https://doi.org/10.1016/j.marchem.2005.05.006

Seyfried, W., Seewald, J., Berndt, M., Ding, K., & Foustoukos, D. (2003). Chemistry of hydrothermal vent fluids from the Main Endeavour Field, northern Juan de Fuca Ridge: Geochemical controls in the aftermath of June 1999 seismic events. *Journal of Geophysical Research*, *108*. https://doi.org/10.1029/2002jb001957

Seymour, J. R., Amin, S. A., Raina, J.-B., & Stocker, R. (2017). Zooming in on the phycosphere: The ecological interface for phytoplankton–bacteria relationships. *Nature microbiology*, *2*, 1–12. https://doi.org/10.1038/nmicrobiol.2017.65

Sharp, J. H., Rinker, K. R., Savidge, K. B., Abell, J., Yves Benaim, J., Bronk, D., et al. (2002). A preliminary methods comparison for measurement of dissolved organic nitrogen in seawater. *Marine Chemistry*, *78*, 171–184. https://doi.org/10.1016/s0304-4203(02)00020-8

Shock, E. L., Oelkers, E. H., Johnson, J. W., Sverjensky, D. A., & Helgeson, H. C. (1992). Calculation of the thermodynamic properties of aqueous species at high pressures and temperatures. Effective electrostatic radii, dissociation constants and standard partial molal properties to 1000°C and 5 kbar. *Journal of the Chemical Society, Faraday Transactions*, *88*, 803–826. https://doi.org/10.1039/ft9928800803

Sipler, R., & Bronk, D. (2015). Dynamics of dissolved organic nitrogen. In D. A. Hansel, & C. A. Carlson (Eds.), *Biogeochemistry of marine dissolved organic matter* (2nd ed., pp. 127–232): Elsevier.

Sirevåg, R., Buchanan, B., Berry, J., & Troughton, J. (1977). Mechanisms of CO_2 fixation in bacterial photosynthesis studied by the carbon isotope fractionation technique. *Archives of Microbiology*, *112*, 35–38.

Smith, D. C., Simon, M., Alldredge, A. L., & Azam, F. (1992). Intense hydrolytic enzyme activity on marine aggregates and implications for rapid particle dissolution. *Nature*, *359*, 139–142. https://doi.org/10.1038/359139a0

Stookey, L. L. (1970). Ferrozine—A new spectrophotometric reagent for iron. *Analytical Chemistry*, *42*, 779–781. https://doi.org/10.1021/ac60289a016

Takai, K., Nunoura, T., Ishibashi, J. i., Lupton, J., Suzuki, R., Hamasaki, H., et al. (2008). Variability in the microbial communities and hydrothermal fluid chemistry at the newly discovered Mariner hydrothermal field, southern Lau Basin. *Journal of Geophysical Research: Biogeosciences*, *113*, 2005–2012.

Tanger, J. C., & Helgeson, H. C. (1988). Calculation of the thermodynamic and transport properties of aqueous species at high pressures and temperatures; revised equations of state for the standard partial molal properties of ions and electrolytes. *American Journal of Science*, *288*, 19–98. https://doi.org/10.2475/ajs.288.1.19

Tanoue, E., & Handa, N. (1979). Distribution of particulate organic carbon and nitrogen in the Bering Sea and northern North Pacific Ocean. *Journal of the Oceanographical Society of Japan*, *35*, 47–62. https://doi.org/10.1007/bf02108282

Taylor, B., Zellmer, K., Martinez, F., & Goodliffe, A. (1996). Sea-floor spreading in the Lau back-arc basin. *Earth and Planetary Science Letters*, *144*, 35–40. https://doi.org/10.1016/0012-821x(96)00148-3

Tupas, L. M., Popp, B. N., & Karl, D. M. (1994). Dissolved organic carbon in oligotrophic waters: Experiments on sample preservation, storage and analysis. *Marine Chemistry*, *45*, 207–216. https://doi.org/10.1016/0304-4203(94)90004-3

Walker, B. D., McCarthy, M. D., Fisher, A. T., & Guilderson, T. P. (2008). Dissolved inorganic carbon isotopic composition of low-temperature axial and ridge-flank hydrothermal fluids of the Juan de Fuca Ridge. *Marine Chemistry*, *108*, 123–136. https://doi.org/10.1016/j.marchem.2007.11.002

Walter, S. R. S., Jaekel, U., Osterholz, H., Fisher, A. T., Huber, J. A., Pearson, A., et al. (2018). Microbial decomposition of marine dissolved organic matter in cool oceanic crust. *Nature Geoscience*, *11*, 334–339.

White, D., Drummond, J., & Fuqua, C. (2012). *The physiology and biochemistry of prokaryotes* (4th ed.). New York, NY: Oxford University Press. ISBN-13: 978-0195393040.

Williams, P. J. L. B. (1970). Heterotrophic utilization of dissolved organic compounds in the sea I. Size distribution of population and relationship between respiration and incorporation of growth substrates. *Journal of the Marine Biological Association of the United Kingdom*, *50*, 859–870. https://doi.org/10.1017/s0025315400005841

Wong, W. W., & Sackett, W. M. (1978). Fractionation of stable carbon isotopes by marine phytoplankton. *Geochimica et Cosmochimica Acta*, *42*, 1809–1815. https://doi.org/10.1016/0016-7037(78)90236-3

Zbinden, M., & Cambon-Bonavita, M. (2020). Rimicaris exoculata: Biology and ecology of a shrimp from deep-sea hydrothermal vents associated with ectosymbiotic bacteria. *Marine Ecology Progress Series*, *652*, 187–222. https://doi.org/10.3354/meps13467

Dickson, A. G. Sabine, C. L. & Christian, J. R. (Eds.), (2007). *Guide to Best Practices for Ocean CO_2 Measurements* (p. 191). PICES Special Publication 3. ISBN: 1-897176-07-4.

Zellmer, K. E., & Taylor, B. (2001). A three-plate kinematic model for Lau Basin opening. *Geochemistry, Geophysics, Geosystems*, *2*. https://doi.org/10.1029/2000gc000106

Zerkle, A. L., House, C. H., & Brantley, S. L. (2005). Biogeochemical signatures through time as inferred from whole microbial genomes. *American Journal of Science*, *305*, 467–502. https://doi.org/10.2475/ajs.305.6-8.467

Zhang, C. L., Ye, Q., Reysenbach, A.-L., Gotz, D., Peacock, A., White, D. C., et al. (2002). Carbon isotopic fractionations associated with thermophilic bacteria Thermotoga maritima and Persephonella marina. *Environmental Microbiology*, *4*, 58–64. https://doi.org/10.1046/j.1462-2920.2002.00266.x

References From Supporting Information

Baumberger, T., Lilley, M. D., Resing, J. A., Lupton, J. E., Baker, E. T., Butterfield, D. A., et al. (2014). Understanding a submarine eruption through time series hydrothermal plume sampling of dissolved and particulate constituents: West Mata, 2008–2012. *Geochemistry, Geophysics, Geosystems*, *15*, 4631–4650. https://doi.org/10.1002/2014GC005460

Bowers, T. S., Campbell, A. C., Measures, C. I., Spivack, A. J., Khadem, M., & Edmond, J. M. (1988). Chemical controls on the composition of vent fluids at 13°–11°N and 21°N, East Pacific Rise. *Journal of Geophysical Research: Solid Earth*, *93*, 4522–4536.

Butterfield, D. A., Jonasson, I. R., Massoth, G. J., Feely, R. A., Roe, K. K., Embley, R. E., et al. (1997). Seafloor eruptions and evolution of hydrothermal fluid chemistry. *Philosophical Transactions of the Royal Society of London Series A-Mathematical Physical and Engineering Sciences*, *355*, 369–386.

Butterfield, D. A., Nakamura, K.-i., Takano, B., Lilley, M. D., Lupton, J. E., Resing, J. A., & Roe, K. K. (2011). High SO_2 flux, sulfur accumulation, and gas fractionation at an erupting submarine volcano. *Geology*, *39*, 803–806.

Campbell, A. C., Bowers, T. S., Measures, C. I., Falkner, K. K., Khadem, M., & Edmond, J. M. (1988). A time series of vent fluid compositions from 21° N, East Pacific Rise (1979, 1981, 1985), and the Guaymas Basin, Gulf of California (1982, 1985). *Journal of Geophysical Research*, *93*, 4537–4549.

Foustoukos, D. I., & Seyfried, W. E. (2004). Hydrocarbons in hydrothermal vent fluids: The role of chromium-bearing catalysts. *Science*, *304*, 1002–1005.

Lang, S. Q., Butterfield, D. A., Schulte, M., Kelley, D. S., & Lilley, M. D. (2010). Elevated concentrations of formate, acetate and dissolved organic carbon found at the Lost City hydrothermal field. *Geochimica et Cosmochimica Acta*, *74*, 941–952.

McCollom, T. M., & Seewald, J. S. (2006). Carbon isotope composition of organic compounds produced by abiotic synthesis under hydrothermal conditions. *Earth and Planetary Science Letters*, *243*, 74–84.

McCollom, T. M., & Seewald, J. S. (2007). Abiotic synthesis of organic compounds in deep-sea hydrothermal environments. *Chemical Reviews*, *107*, 382–401.

McDermott, J. M., Seewald, J. S., German, C. R., & Sylva, S. P. (2015). Pathways for abiotic organic synthesis at submarine hydrothermal fields. *Proceedings of the National Academy of Sciences of the United States of America*, *112*, 7668–7672.

Michard, A., Albarede, F., Michard, G., Minster, J., & Charlou, J. (1983). Rare-earth elements and uranium in high-temperature solutions from East Pacific Rise hydrothermal vent field (13 N). *Nature*, *303*, 795–797.

Rouxel, O., Shanks, W. C., III, Bach, W., & Edwards, K. J. (2008). Integrated Fe- and S-isotope study of seafloor hydrothermal vents at East Pacific Rise 9–10°N. *Chemical Geology*, *252*, 214–227.

Seewald, J. S., Zolotov, M. Y., & McCollom, T. (2006). Experimental investigation of single carbon compounds under hydrothermal conditions. *Geochimica et Cosmochimica Acta*, *70*, 446–460.

Shock, E. L. (1990). Geochemical constraints on the origin of organic-compounds in hydrothermal systems. *Origins of Life and Evolution of the Biosphere*, *20*, 331–367.

Shock, E. L. (1992). Chemical environments of submarine hydrothermal systems. In N. G. Holm (Ed.), *Marine Hydrothermal Systems and the Origin of Life*. Dordrecht: Springer. https://doi.org/10.1007/978-94-011-2741-7_5

Summit, M., & Baross, J. A. (1998). Thermophilic subseafloor microorganisms from the 1996 North Gorda Ridge eruption. *Deep Sea Research Part II: Topical Studies in Oceanography*, *45*, 2751–2766.

Von Damm, K. (1990). Seafloor hydrothermal activity: Black smoker chemistry and chimneys. *Annual Review of Earth and Planetary Sciences*, *18*, 173.

Von Damm, K. L., Edmond, J. M., Grant, B., Measures, C. I., Walden, B., & Weiss, R. F. (1985). Chemistry of submarine hydrothermal solutions at 21°N, East Pacific Rise. *Geochimica et Cosmochimica Acta*, *49*, 2197–2220.

Von Damm, K. L., Lilley, M. D., Shanks, W. C., Brockington, M., Bray, A. M., O'Grady, K. M., et al. (2003). Extraordinary phase separation and segregation in vent fluids from the southern East Pacific Rise. *Earth and Planetary Science Letters*, *206*, 365–378.

Von Damm, K. L., Parker, C. M., Lilley, M. D., Olson, E. J., Clague, D. A., Zierenberg, R. A., & McClain, J. S. (2006). Chemistry of vent fluids and its implications for subsurface conditions at Sea Cliff hydrothermal field, Gorda Ridge. *Geochemistry, Geophysics, Geosystems*, *7*. https://doi.org/10.1029/2005GC001034